Water Air Soil Pollut (2026) 237:564
https://doi.org/10.1007/s11270-026-09202-z

Pollutant Lead Mobility in Forest Soils of the Northeastern United States Evaluated with a 40-Year Resampling Study

Justin B. Richardson · Owen C. Porterfield · Andrew W. Schroth · Andrew J. Friedland · James M. Kaste

Received: 30 August 2025 / Accepted: 23 January 2026

Abstract Lead (Pb) is a toxic metal that was dispersed by humans worldwide largely through Pb gasoline combustion. Regional scale long-term datasets detecting changes and processes governing pollutant Pb pools are exceedingly rare. Here, we evaluated changes in forest floor (Oie + Oa) Pb from 1980–2021, differences in mineral soil Pb with depth (0–10, 10–20, 20 -30, and 30–50 cm), and variations in foliar and litterfall Pb at seventeen sites across the northeastern US. Forest floor Pb concentrations and pools have further decreased by 65 to 87% with forest floor Pb concentration response time (*TrespC*) of 35 years. The correlation between *TrespC* with the soil organic matter, site latitude, and site longitude highlights that colder sites have slower forest floor turnover that in turn promotes Pb retention. Forest floor Pb desorption was greatest for circumneutral organic ligands and mineral soil partition coefficient (Kd) varied among subregions and decreased with depth. Overall mineral soil Pb concentrations were 14.3 ± 2.2 mg kg^{-1} and mineral soil amounts (top 50 cm) were 27 ± 2.2 kg ha^{-1}. Seven forest floor Oa horizons still exceed ecological screening levels for impacting wildlife. Foliar Pb concentrations did not vary among genera nor correlated with soil concentrations. Estimated Pb litterfall fluxes (1 to 4 g ha^{-1} yr^{-1}) were < 1% of the current forest floor pool, highlighting uptake discrimination against Pb. Our study highlights the power of sustained long-term repeated decadal measurements of legacy Pb to quantify changes and variation at a regional scale.

Keywords Forest floor · Mineral soil · Spodosols · Pb biogeochemistry · Toxic metal

Supplementary Information The online version contains supplementary material available at https://doi.org/10.1007/s11270-026-09202-z.

J. B. Richardson (✉)
Department of Environmental Sciences, University of Virginia, Clark Hall 291 McCormick Rd, Charlottesville, VA 22904, USA
e-mail: Justin.Richardson@virginia.edu

J. B. Richardson · O. C. Porterfield
Department of Geosciences, University of Massachusetts Amherst, Amherst, MA 01003, USA

A. W. Schroth
Department of Geography and Geosciences, University of Vermont, Burlington, VT, USA

A. J. Friedland
Department of Environmental Studies, Dartmouth College, Hanover, NH 03755, USA

J. M. Kaste
Department of Geology, William & Mary, Williamsburg, VA 23185, USA

1 Introduction

Lead (Pb) is a non-essential, toxic element that was widely released across the northeastern United States.

Published online: 18 February 2026

Its long-term impacts remain on terrestrial ecosystems and movement to groundwater and streams remains uncertain. From roughly 1930 to 1980, Pb was released across the northeastern US region, primarily through the combustion of Pb gasoline and coal (Duruibe et al., 2007; Levin et al., 2021; Sarkar et al., 2015), but also localized smelting (e.g. Ketterer et al., 2001), industrial manufacturing (Caballero-Gómez et al., 2022; Tuccillo et al., 2023), and municipal waste incineration (Bogush et al., 2019; Walsh et al., 2001; Wei et al., 2022). Atmospheric Pb deposition in the northeastern US peaked between 1973 and 1978 at an estimated rate of 147 to 396 g ha^{-1} yr^{-1} (Johnson et al., 1995; Richardson et al., 2014; Sarkar et al., 2015). By 2007, the rate of atmospheric Pb deposition across the region had fallen to an estimated range of 6.5 to 90 g ha^{-1} yr^{-1} (Richardson et al., 2015; Sarkar et al., 2015). Regional decreases in atmospheric Pb deposition are largely credited to the gradual phase out of Pb gasoline beginning in late 1973 and the passage of the Clean Air Act in 1977 and Clean Air Act 1990 Amendments (Johnson et al., 1995; Miller & Friedland, 1994; Nadim et al., 2001; Wade et al., 2021). The reduction in atmospheric Pb has positively impacted the quality of health and economic output across America (e.g. Isen et al., 2017). Nevertheless, the magnitude and impacts of Pb residence and sequestration in terrestrial impacts remain unclear with fewer studies evaluating Pb movement in non-urban areas.

Forest sites located across the northeastern US are terrestrial sinks for much of this atmospheric Pb deposition through their forest floor (combined organic horizon layers of Oi, Oe, Oa) (Johnson et al., 1982a, 1982b; Friedland et al., 1984; Siccama & Smith, 1978; Richardson et al., 2014) and mineral soil horizons (Richardson et al., 2014; Smith & Siccama, 1981). The forest floor has been shown to have a high sorption capacity for Pb due to its high soil organic matter (SOM) content and abundance of mineral surfaces (Kaste et al., 2005; Kabata-Pendias and Mukherjee, 2007; Richardson et al., 2014; Schroth et al., 2008; Zhao et al., 2024). Following deposition to the forest floor, Pb is generally insoluble and binds to SOM, amorphous Fe oxyhydroxides, and other mineral surfaces, thus soils with higher SOM and Fe oxide content generally caused higher metal adsorption (Kaste et al., 2005; Richardson et al., 2014; Schroth et al., 2008; Yang et al., 2022; Zheng et al., 2022). However, as this SOM gradually decomposes over time and microbial communities interact with mineral surfaces, Pb is expected to be redistributed to lower depths in the soil profile and potentially enter ground or surface waters (Kaste et al., 2005; Richardson et al., 2014; Schroth et al., 2008; Zhang et al., 2021). Due to the complexity of abiotic and biotic processes occurring in soils that can both promote leaching and retention, continued field studies are needed to determine the rate of Pb fluxes in the forest floor and mineral soil.

Retention of Pb in the forest floor and surface mineral soil allows for elevated Pb concentrations that can negatively impact plants, soil dwelling organisms, and soil invertebrate consumers (Morales-Silva et al., 2024; Peterson et al., 2024; Šerić Jelaska et al., 2014). Pollutant Pb adsorbed to organic matter can be transferred to saprotrophic feeders and their predators. For example, predatory beetles can accumulate metals including Pb from consuming saprotrophic litter feeders such as earthworms, slugs, springtails, and wood life, which can be transferred to avian consumers (Šerić Jelaska et al., 2014). For this reason, the U.S. EPA introduced Ecological Soil Screening Levels (Eco-SSLs) that define concentrations that can impact soil invertebrates, birds, mammals, and plants using ecotoxicological studies that met rigorous criteria (USEPA, 2005). Soil Pb concentrations of 56 mg kg^{-1} and greater can negatively impact wildlife (USEPA, 2005). To directly harm soil invertebrates, Eco-SSLs for Pb were estimated to be 1700 mg kg^{-1} before direct harm to the arthropods and gastropods occurred. In addition to animal uptake, soil Pb can be taken up by plants via rhizosphere biogeochemical processes of biological, organo-chelation, and abiotic desorption (Albert et al., 2020; Liu et al., 2023; Rahman et al., 2024). Soil Pb concentrations of $\geq$ 120 mg kg^{-1} can negatively impact terrestrial plant growth and reproduction (USEPA, 2005). However, it must be noted that Pb retention in soil below the rooting zone can be viewed as an ecosystem service of protecting groundwater and surface waters from contamination (e.g. Ding et al., 2018).

This study builds upon a 40-yr forest soil resampling in the eastern US by adding green leaf Pb concentrations, separating different stage decomposed forest floor material (Oie vs Oa), and deeper mineral soil sampling with new analysis of partition coefficients (Kd). By adding these new measurements, we

address three objectives to establish both the current state of legacy Pb pollution and biotic-abiotic processes governing Pb cycling dynamics within forests on mountains across the northeastern United States. Objective 1 was to evaluate if inputs of new litter that is relatively depleted in atmospheric Pb is driving lower forest floor Pb concentrations and amounts from 1980 to 2021 and if this process varies among three climatic subregions. Objective 2 was to evaluate downward mineral soil Pb movement using concentration profiles and sorption capacity and determine if Pb movement varies by site-specific properties (across the 17 research sites) or by regional climate processes across the three subregions. We expected that mineral soil Pb would remain primarily in the top 10 cm of the mineral soil due to ample retention by available Fe oxide and organic Pb-complexes, and forest floor desorption to be driven by cumulative effects of acidity, chelation, and base cation exchange, and mineral soil sorption associated with Fe oxides and organic matter. Objective 3 was to compare 2021 foliar Pb concentrations and amounts in order to establish whether the role of aboveground Pb cycling by trees to determine the rate of biological uptake by trees and if this varies with site-specific properties across the seventeen research sites, with climate among the three subregions, or if it is species-specific among the eight main tree genera across the study region.

2 Materials and Methods

2.1 Re-Sampling Seventeen Sites

We have re-sampled seventeen upland long-term research sites, established in 1980 across the northeastern United States as part of a larger study examining Pb in the forest floor (Johnson et al., 1982a, 1982b; Friedland et al., 1992; Kaste et al., 2006; Richardson et al., 2014; Supplemental Table 1). The sites were all established in 1980 and situated in undisturbed forests generally located at higher elevations (Fig. 1, Table 1), with many sites within State and National research forests (Johnson et al., 1982a, 1982b; Friedland et al., 1992; Kaste et al., 2006; Richardson et al., 2014). The seventeen sites were relocated during the summer of 2021 using GPS and instructions. Sites were grouped into the same three subregions as Richardson et al. (2014): western, central, and northern (Table 1).

Soils at the seventeen forest research sites were formed from glacial till, outwash deposits, or outcrops of weathered bedrock (Kaste et al., 2006). Site soils are well-drained and were sampled on level to shallow slopes less than 8%. Soils were classified in the field using the USDA soil taxonomy guidelines (Soil Survey Staff, 2022), with all sites being classified as either Spodosols or Inceptisols except for Sites #1 and #3, which were classified as Ultisols. As a general trend, northern sites were Spodosols, central sites were Inceptisols, and western sites were Ultisols. To ensuring comparability, the forest floor mass and %LOI across resampling are shown in Supplemental Figure S2 and 2021 data are provided in Supplemental Table S2.

2.2 Vegetation Samples and Forest Canopy Calculation

Vegetation at each site is mixed; sites ranged from primarily deciduous vegetation such as oak (*Quercus* spp.), American beech (*Fagus* spp.), maple (*Acer* spp.), and birch (*Betula* spp.), to primarily coniferous vegetation such as pine (*Pinus* spp.), spruce (*Picea* spp.), hemlock (*Tsuga* spp.), and balsam fir (*Abies balsamea*) (Table 1). Northern sites were generally dominated by coniferous vegetation, while central and western sites were generally dominated by deciduous vegetation.

Tree species were identified in 1980 but the size and stem densities were measured in 2021. At each site, a circular 750 m^2 plot size encompassing the tree and soil sampling locations were identified and measured for diameter at breast height (DBH at 1.3 m). Aboveground woody biomass and foliar biomass was estimated using allometric equations for each species from studies conducted in the northeastern US and southeastern Canada (Jenkins et al., 2003; Ter-Mikaelian & Korzukhin, 1997). The foliar and woody biomass for each tree was summed for an estimate of total foliar and woody biomass at each stand. Estimates for foliage, aboveground woody biomass, and litterfall were based on allometric equations and parameters from Ter-Mikaelian and Korzukhin (1997) using field measured DBH empirical data. It should be noted that aboveground woody biomass and foliage biomass can vary with canopy geometry, tree morphology, and

Table 1 Location, precipitation, vegetation, and soil characteristics of the seventeen sampled sites. Trees are in order of %basal area abundance for the 750 m^2 plot at each site. Woody biomass, foliar biomass, and annual litterfall fluxes are estimated using allometric equations from measured DBH and species-specific parameters from Ter-Mikaelian & Korzukhin (1997)

Subregion	Site #	Site Name	Elevation	Mean Annual Precipitation†	Vegetation (%)	Median DBH	Woody biomass	Foliar biomass	Estimated Litterfall fluxes
			(m)	(mm yr^{-1})		cm	Mg ha^{-1}	Mg ha^{-1}	Mg ha^{-1} yr^{-1}
Western	1	Heart's Content, PA	580	1170	Hemlock(43)/ Beech(33)/ Birch(24)	38	283	9.2	6.0
Western	2	Cook's Forest, PA	430	1163	Hemlock(61)/ Hickory(19)/ Beech(11)	32	198	5.9	2.9
Western	3	Tionesta, PA	520	1141	Oak(81)/ Pine(16)	43	231	7.0	3.0
Central	4	Balsam Lake, NY	820	1268	Maple(46)/ Birch(29)/ Hickory(24)	29	103	1.8	1.8
Central	5	Mohonk, NY	366	1288	Oak(59)/ Hemlock(39)	28	126	5.3	1.4
Central	6	Mt. Tremper, NY	305	1365	Birch(51)/ Maple(28)/ Beech(10)	27	103	3.0	2.8
Central	7	Windham, NY	580	1215	Oak(49)/ Maple(48)	21	124	2.7	2.4
Central	8	Mohawk Mt., CT	503	1192	Oak(77)/Hickory(17)	20	65	1.4	1.4
Central	9	Mt. Everett, MA	790	1276	Oak(60)/Pitch Pine(24)/ Maple(16)	19	21	0.8	0.6
Northern	10	Appalachian Gap, VT	778	1533	Birch(67)/ Spruce(15)/ Fir(11)	17	62	1.9	1.5
Northern	11	Sherburne Pass, VT	671	1467	Birch(55)/ Maple(29)/ Beech(16)	24	141	2.8	2.8
Northern	12	Bromley, VT	625	1465	Birch(83)/ Maple(11)	34	81	2.2	2.1
Northern	13	Bristol Cliffs, VT	555	1112	Pine(55)/ Hemlock(19)/ Maple(12)	19	18	0.8	0.4
Northern	14	Mt. Cardigan, NH	579	1306	Spruce(78)/ Birch(12)/ Fir(10)	30	82	5.9	1.6
Northern	15	Valley Way, NH	433	1217	Beech(55)/ Birch(28)/ Hemlock(10)	25	185	4.0	3.4

Table 1 (continued)

Subregion	Site #	Site Name	Elevation	Mean Annual Precipitation†	Vegetation (%)	Median DBH	Woody biomass	Foliar biomass	Estimated Litterfall fluxes
Northern	16	Gale River, NH	440	1181	Spruce(46)/ Birch(40)/ Beech(10)	25	74	3.0	1.4
Northern	17	Wildcat Mt, NH	590	1527	Maple(59)/ Spruce(22)/ Fir(19)	16	45	2.4	1.1

† Precipitation values interpolated from PRISM database (PRISM Climate Group, 2023)

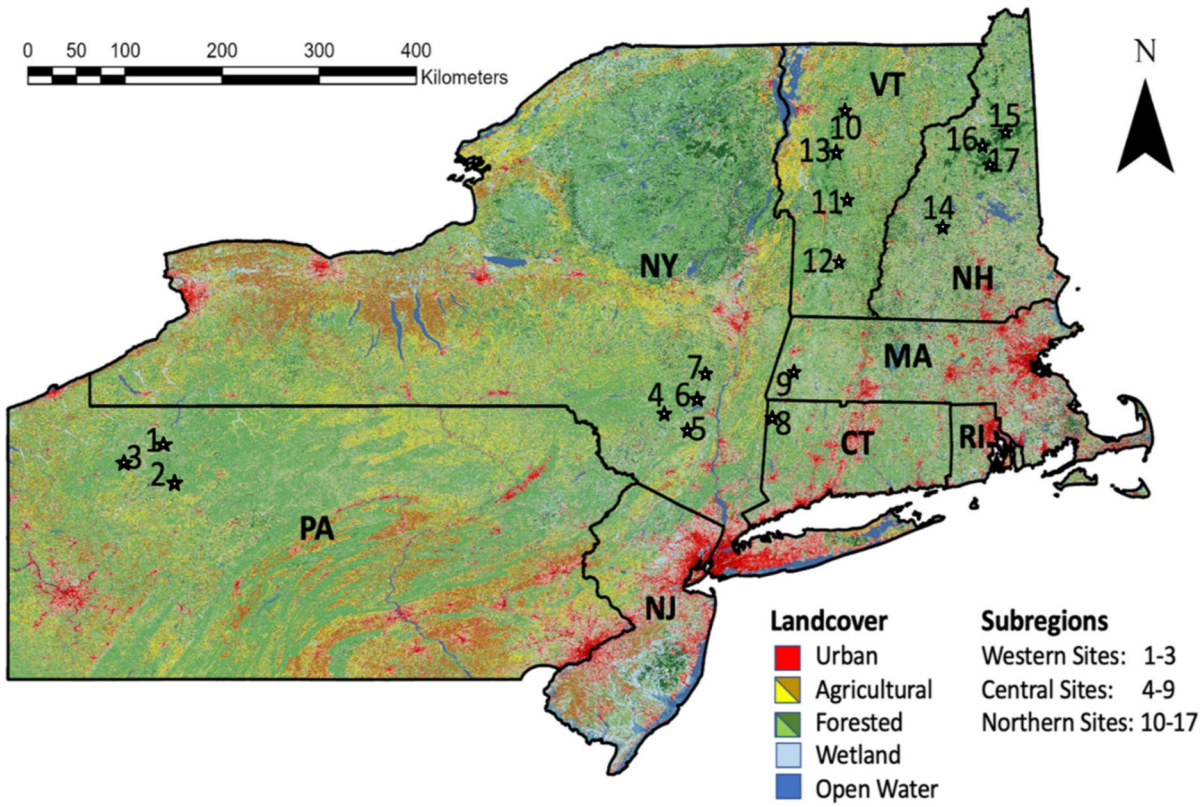

Fig. 1 Locations of the seventeen soil research sites overlaid on 2018 National Landcover Database (Dewitz 2021)

fitness of each tree (Ferrari & Sugita, 1996; Luyssaert et al., 2002). Late-summer green leaves from dominant tree species present were sampled using either an arborist throw-ball to strip off small branches and leaves or if the mid-canopy was low enough, branches and leaves were cut using pole pruners. We estimated litterfall rates for each individual tree at each plot following Richardson and Friedland (2016), where 100% of foliage from deciduous trees were expected to senesce while only 33% of fir and pine needles and 20% of spruce and hemlock needles were expected to senesce (see Augusto et al., 2015). Summing all individual tree litter was then used to estimate site level litterfall mass (Table 1) and using the late-season leaf Pb concentrations for each tree species at each site, we estimated site level litterfall Pb fluxes.

2.3 Soil Sample Collection and Processing

Forest floor and mineral soil samples were collected from each of the seventeen sites between June and August of 2021. Five forest floor and three mineral soil cores were taken at each site in a 30 m × 30 m area. The five forest floor was collected using the same method used by Johnson et al. (1982a), Friedland et al (1992), Kaste et al. (2006), and Richardson et al. (2014). In brief, five 15 cm × 15 cm sections of randomly chosen forest floor were cut and removed from the underlying mineral soil at each site. Instead of analyzing the forest floor as a whole, each forest floor sample was divided into two subsamples by hand into the combined partially-decomposed leaf litter, high fibrous material content as Oie horizons, and the highly-decomposed, low fibrous content Oa horizon, which better alights with methods used at other locations such as Hubbard Brook Experimental Forest (e.g. Johnson et al., 1995). We utilized the USDA NRCS Field Book for Describing and Sampling Soils and used fibrous content to separate Oe and Oa horizon materials. Roots > 1 cm were removed and the forest floor was milled to < 2 mm.

Mineral soil samples were obtained using an auger and intact soil cores at three of the five forest floor sampling locations. The 2021 soil cores were collected for the following four mineral soil depths; 0–10 cm, 10–20 cm, 20–30 cm, and 30–50 cm. Depths were ensured using a measuring rod. Mineral soil samples do not capture the belowground variability in bulk soil and rock fragment fractions as shallow soils with lithic contact were not sampled. Due to the topography and slope position, mineral soils were generally shallow (< 1 m deep) and 30–50 cm depths were unable to be collected at Sites #4, 6, 7, 10 and 17 due to high rock content or the presence of a hardpan layer (Richardson et al., 2014). Mineral soil samples were dried and sieved to < 2 mm. Bulk density of the mineral soil was determined using the intact soil cores for the depth intervals sampled using a 15 cm diameter steel cylinder hammered into the mineral soil following the same methods as Richardson et al (2014).

Forest floor and mineral soil samples were analyzed for pH using 0.01 M calcium chloride ($CaCl_2$) at a 2:15 soil:$CaCl_2$ gravimetric ratio then measured via a pH probe. Soil organic matter content (SOM %) was determined for the forest floor and mineral soil samples through loss on ignition. Soil particle size distribution was determined for the mineral soil samples using a modified Bouyoucos hydrometer method using hydrometer readings were taken at 60 s and 1.5 h.

2.4 Forest Floor Pb Desorption Rreactions

To quantify forest floor desorption mechanisms and its variability across forest soils, we utilized batch equilibration technique across a combination of acidity (acid), dissolved organic ligand (DOL), and base cation salt exchange (salts) treatments. For the acid treatment, trace metal grade nitric acid was diluted to pH 3 to simulate acidity from roots and decomposition. For the DOL treatment, we used the most and least effective low molecular weight organic ligands of citrate and acetate (Zhang et al., 2022) at 50 mM citrate and 50 mM acetate solution at pH 6.8 to simulate DOL released from decomposing plant litter. For the salts treatment, the solution consisted of 50 mM Ca, 50 mM Mg, 50 mM K, and 50 mM Na solution at pH 6.8 to simulate cations added to the soil from plant material, dust, and mineral weathering. We examined combined treatment effects because the combination of the conditions commonly occur in soils compete or negate impacts on forest floor Pb desorption (e.g. Zhang et al., 2022). The first combination was strong acidity with organic ligands (acid + DOL) for a 50 mM citrate and 50 mM acetate solution at pH 3. The second combination was base cation salts added with organic ligands (salt + DOL) at pH 6.8. A final combined treatment of acidity, base cation salts, and organic ligands (acid + salt + DOL) was explored as the potential mechanism that may promote the greatest forest floor Pb desorption via cation exchange, proton-promoted desorb, and increased solubility from chelation. For the experiment, 1 g of forest floor was weighed into an acid-washed 50 mL centrifuge tube and mixed with 30 g of treatment solution in triplicate. The tubes were closed and continuously shaken for 48 h at 25 °C then allowed to settle for 12 h. The slurry was centrifuged at 2800 rpm for 30 min and the supernatant was removed. A 0.5 g subsample was filtered to < 0.45 µm, digested with 1 to 8 g of 30% H_2O_2 to remove organics that can affect the plasma ionization, and acidified to 15 g with 2% nitric acid and measured with an Agilent 7900 Inductively Coupled Plasma Mass Spectrometry (Agilent

Technologies, Santa Clara CA USA). The amount of desorbed Pb measured was normalized to the original mass of forest floor Pb.

2.5 Mineral Soil Pb Sorption

To quantify the variation in Pb retention across forest soils, adsorption isotherms were measured using a series of batch reactors for solid and aqueous partitioning for the 0–10 cm depth and 30 to 50 cm depths only. In brief, we utilized five treatment levels using trace metal grade $Pb(NO_3)_2$ at 0, 5, 50, 100, and 500 mg L^{-1} and diluted with 100 mg L^{-1} $NaNO_3$ to maintain ionic strength. The initial Pb solution was adjusted to pH 5.0 by adding 0.5 mol L^{-1} HNO_3 solutions but was not adjusted once added to the soils. For the reaction, 2 g of soil with 20 mL of solution in acid washed 50 mL centrifuge tubes. The tubes were closed and continuously shaken for 48 h at 25 °C. Coarse particles were allowed to settle over 12 h to achieve near steady state (see Park et al., 2019) and the slurry was centrifuged at 2800 rpm for 30 min and the supernatant was removed and filtered to < 0.45 µm. A 0.5 g subsample was acidified to 15 g with 2% nitric acid. To determine the phase partitioning coefficient (K_d), the concentration of solid phased Pb (q) and concentration remaining in solution (C) was calculated by fitting the Freundlich equation (**Eq.** 1) using MATLAB Curve Fitter tool.

$$q = K_d \times C^{(1/n)} \quad (1)$$

2.6 Pb Elemental Analyses

A modified version of the U.S. EPA method 3050B following protocols similar to Johnson et al., (1982a, 1982b) and Friedland et al. (1992) were used to measure the concentration of Pb in forest floor, foliage, and mineral soil samples through strong acid digestion. Prior to digestion, 5.0 ± 0.1 g of forest floor, 0.5 ± 0.1 g of foliage, and 0.5 ± 0.1 g of litterfall samples were weighed into crucibles and ashed in a muffle furnace at 550 ℃ for a minimum of 8 h to remove organic matter. The ash was transferred to 50 mL centrifuge tubes for digestion. For mineral soil samples, 2.0 ± 0.1 g were digested directly within the 50 mL centrifuge tubes. Samples were digested with 5 mL of a 9:1 ratio of trace metal grade nitric acid:hydrochloric acid (HNO_3, 70%; HCl, 36%) and then heated to 80 ºC for 45 min under sealed conditions. Upon cooling, digested samples were diluted to a volume of 50 mL with 18.2 MΩ deionized water and 5 g subsample was further diluted to 15 mL. For every 30 digested samples, one preparation blank and two standard reference materials (SRM) were included. Similarly, for every 20 digested foliage samples, one preparation blank and one SRM was included. Peach Leaves 1547 and San Joaquin 2709a from the National Institute of Standards and Technology (National Institute of Standards and Technology Gaithersburg, MD) were used as reference certified Pb values. Preparation blanks were < 0.87 µg kg^{-1}, and all measured Pb concentrations for SRM materials were within ± 9.12% of their certified values with an Agilent 7700 × Inductively Coupled Plasma-Mass Spectrometer.

2.7 Data Analyses and Statistical Tests

Descriptive statistics for Pb and soil properties were calculated using and MATLAB (MathWorks, Natick, MA). Mean Pb concentrations and amounts and soil property values are given ± 1 standard error in the text, tables, and figures included in this paper. Wilcoxon rank-sum test was used to identify statistically significant differences between mean values in all analyses pertaining to only two groups. The Kruskal Wallis Test was used to identify statistically significant differences between the mean values of three or more groups in all corresponding cases. Correlative relationships between Pb concentrations with geographic factors (latitude, longitude, elevation, and mean annual precipitation) and soil physicochemical properties (% SOM, pH, and Fe concentration,) were evaluated using stepwise regressions and multiple regression in Matlab. Due to the shared bulk density used to determine Pb, Fe, and SOM amounts, correlations, stepwise regressions, and multiple regressions were not performed.

Changes in Pb concentrations and amounts from 1980 to 2021 were evaluated using an exponential regression function (**Eq.** 2) in Matlab to empirically describe Pb at a given time between 1980 and 2021 [Pb_t] from a starting level in 1980 [Pb_0] (Mathworks, Natick, MA). Using the calculated the rate constant, k, from the slope of the exponential regressions, we calculated a response time using concentration as

previously conducted by Richardson et al. (2014), *TrespC*, to describe the retention time for Pb in the forest floor based upon concentrations. We also calculated we calculated a response time using amounts as previously conducted by Miller and Friedland (1994), *TrespA*, to describe the retention time for Pb in the forest floor based upon amounts. The *Tresp* parameters are the time required for a pulse to move through a reservoir not in steady state assuming Pb in the forest floor can be described as a first-order rate process (**Eq.** 3) and was empirically-calculated using the k values with **Eq.** 4 (Miller & Friedland, 1994; Watmough & Hutchinson, 2004).

$$[Pb_t] = [Pb_0]e^{-kt} \tag{2}$$

$$d[Pb]/dt = -k \tag{3}$$

$$Tresp = \frac{1}{k} \tag{4}$$

3 Results

3.1 Pb in the Forest Floor—2021 Sampling

Overall, forest floor Pb concentrations and amounts have continued to decrease over time, with greater losses in the western than northern among the subregions following differences in climate and physicochemical properties. Forest floor Pb concentrations in 2021 ranged from 8 to 152 mg kg^{-1} across all sites with a region-wide average of 43 ± 9 mg kg^{-1}. Mean forest floor Pb concentrations in 2021 were significantly higher in central sites than in both western and northern sites ($p < 0.05$; Fig. 2; Supplemental Figure S1). Average forest floor Pb concentrations across the northeastern United States have declined significantly ($p < 0.05$) between 1980 and 2021 with an overall decrease of $72\% \pm 4\%$ (Fig. 2). More recently, the entire study region declined significantly ($p < 0.05$) between 2011 and 2021 a decrease of 37%. Physicochemical properties of the forest floor and site location data are included in Supplemental Table S2. Forest floor mass ranged between 15 to 399 Mg ha^{-1} with an average of 96 ± 21 Mg ha^{-1}, %SOM ranged between 55 to 91% with an average of $76 \pm 2\%$, forest floor thickness ranged between 2.2 to 24.4 cm with an average of 21 ± 3 cm, and lastly forest floor pH ranged between pH 2.7 to 4.5 with an average of pH 3.4 ± 0.5. Forest floor Pb concentrations were found to be significantly correlated with latitude, longitude, elevation, %SOM, and pH with linear regressions ($R^2 > 0.20$; $p < 0.05$; Supplemental Figure S3) and when multiple-regressed with geographic and physicochemical variables (Table 2).

Forest floor Pb amounts in 2021 ranged from 0.1 to 16 kg ha^{-1} across all sites with a region-wide average of 4.4 ± 1.1 kg ha^{-1}, which is significantly lower than the forest floor Pb amounts in 1980 of 15.6 ± 2.8 kg ha^{-1} and in 2011 of 7.2 ± 1.4 kg ha^{-1} using paired t-tests ($p < 0.05$). Mean forest floor Pb amounts were significantly higher in northern and central sites than in western sites ($p < 0.05$; **Supplemental** Figure S1), a slightly different trend relative to Pb concentration. Forest floor Pb amounts also declined significantly ($p < 0.05$) across the entire study region from 1980 to 2021 for each study area using Wilcoxon rank-sum test (Fig. 2).

Following the same methodology as Richardson et al. (2014), we calculated the exponential decay rate mean Pb response time for all sites through 1980, 1990, 2002, 2011, and 2021 for forest floor Pb concentrations (*TrespC*; Table 3) and forest floor Pb amounts (*TrespA*; Table 3). Decreases in forest floor Pb concentrations at each site were modeled by an exponential regression (**Eq.** 2) with R^2 values > 0.70 for fourteen of the seventeen sites and all sites had an R^2 value > 0.50. The rate constants from the exponential regressions k had a mean value of 0.034 ± 0.003 yr^{-1}, which were larger than the Richardson et al. (2014) estimate of 0.027 ± 0.003 yr^{-1}. The mean Pb response time using forest floor concentrations (*TrespC*) for all sites was 34 ± 4 yr, which was shorter than the Richardson et al. (2014) estimate of 46 ± 7 yr but not significantly shorter.

Decreases in forest floor Pb amounts at each site were also modeled by an exponential regression (**Eq.** 2**,** Table 3) with R^2 values > 0.70 for eleven of the seventeen sites but unfortunately five sites had an R^2 value < 0.60. Site 9 was not significant and had an $R^2 < 0.01$ and was not included in calculations, analyses, nor interpretations. The mean forest floor Pb amount *TrespA* for all sites was 35 ± 7 yr, which matches the forest floor Pb concentration *TrespA*. The *TrespA* parameter was not calculated by Richardson et al. (2014) for forest floor Pb amounts due to most

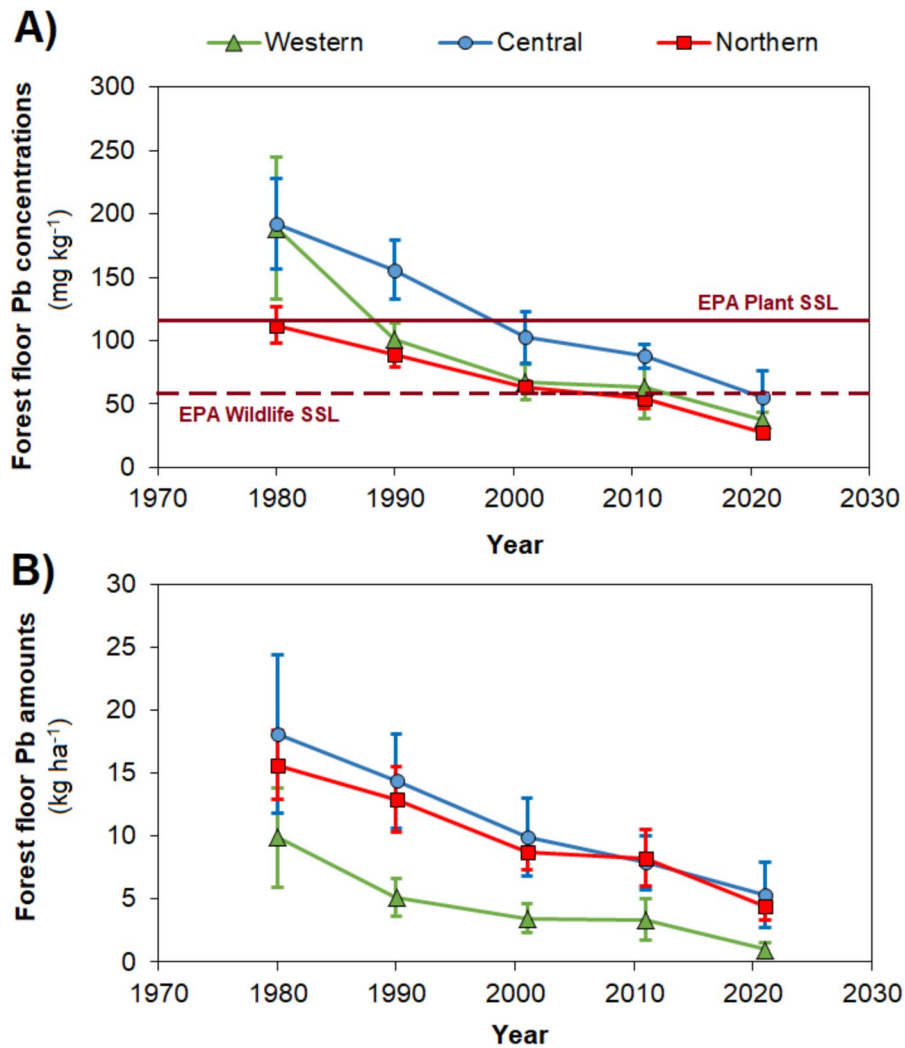

Fig. 2 Forest floor Pb concentrations and amounts (± 1 standard error) are shown for each subregion with previous data from Johnson et al., (1982a, 1982b), Friedland et al (1992), Kaste et al. (2006), Richardson et al (2014) and this study. USEPA Pb plant Eco-SSL of 120 mg kg^{-1} and USEPA Pb mammalian Eco-soil screening level (SSL) of 56 mg kg^{-1} are provided

Table 2 Calculated multiple linear regression model outputs for region-wide 2021 Pb concentrations using significant geographic and physicochemical variables (($R^2 > 0.20$; $p < 0.05$) from a bidirectional stepwise-regression model. The marker (-) indicates a negative relationship between pH and the given metal inventory

Soil Depth	Pb Concentrations Stepwise Linear Regression Significant Variables	Multiple regression R^2
Forest Floor	Latitude, longitude, elevation, %SOM, and pH (-)	0.41
t_{respC}	Latitude, Pb concentration, and %SOM	0.61
Mineral Soil: 0–10 cm	Latitude and %SOM	0.59
Mineral Soil: 10–20 cm	Latitude, longitude, and %SOM	0.54
Mineral Soil: 20–30 cm	Latitude and elevation	0.41
Mineral Soil: 30–50 cm	Latitude, elevation, pH (-), and %SOM	0.49

Table 3 Forest floor Pb amounts (±1 standard error) for the seventeen sampling sites for the years 1980, 1990, 2002, 2011, and 2021

Subregion	Site #	Site Name	Forest floor Pb concentration rate constant	R^2	$T_{resp}C$	Forest floor Pb amount rate constant	R^2	$T_{resp}A$
			yr^{-1}		yr	yr^{-1}		yr
Western	1	Heart's Content, PA	−0.044	0.83	23	−0.0619	0.85	16
Western	2	Cook's Forest, PA	−0.042	0.99	24	−0.0404	0.98	25
Western	3	Tionesta, PA	−0.052	0.95	19	−0.0666	0.85	15
Central	4	Balsam Lake, NY	−0.047	0.79	21	−0.0510	0.77	20
Central	5	Mohonk, NY	−0.025	0.99	41	−0.0254	0.99	39
Central	6	Mt. Tremper, NY	−0.038	0.69	27	−0.0415	0.68	24
Central	7	Windham, NY	−0.049	0.80	20	−0.0489	0.80	20
Central	8	Mohawk Mt., CT	−0.027	0.67	37	−0.0381	0.59	26
Central	9	Mt. Everett, MA	−0.020	0.79	50	-	0.03	-
Northern	10	Appalachian Gap, VT	−0.030	0.93	33	−0.0323	0.95	31
Northern	11	Sherburne Pass, VT	−0.063	0.93	16	−0.0839	0.86	12
Northern	12	Bromley, VT	−0.020	0.82	49	−0.0318	0.88	31
Northern	13	Bristol Cliffs, VT	−0.033	0.83	30	−0.0437	0.76	23
Northern	14	Mt. Cardigan, NH	−0.020	0.66	51	−0.0152	0.47	66
Northern	15	Valley Way, NH	−0.023	0.87	44	−0.0289	0.83	35
Northern	16	Gale River, NH	−0.016	0.90	64	−0.0079	0.43	127
Northern	17	Wildcat Mt, NH	−0.024	0.51	42	−0.0193	0.52	52

‡ Significant difference between 2011 and 2021 ($P < 0.05$) using Wilcoxon

models not producing significant exponential regressions. Forest floor Pb *TrespA* for western and central sites were 19 ± 3 yr and 26 ± 3 yr, respectively, which were not significantly different than *TrespC* estimates for western and central sites. Northern sites had the longest *TrespA* at 47 ± 13 yr, which was not longer than northern sites *TrespC* estimate.

The relationship between *TrespC, TrespA*, and other physicochemical and geographic site properties were investigated using stepwise regressions followed by multiple regression of the significant variables. Forest floor %SOM, site latitude, and 2021 Pb concentration were significantly correlated with *TrespC* ($R^2 > 0.50$, $p < 0.05$) and when combined through multiple regression were able to explain 61% of the variation in *TrespC* (Table 3).

3.2 Forest Floor—Oie and Oa Horizons

Forest floor 2021 samples were subdivided into their subcomponent Oie and Oa horizons and analyzed for Pb, showing recent litter has less Pb but well-above zero. Lead concentrations in the Oie horizon across all sites ranged from 6 to 103 mg kg^{-1}, and an average of 30 ± 3 mg kg^{-1} while Oa horizon across all sites ranged from 11 to 204 mg kg^{-1}, and an average of 57 ± 6 mg kg^{-1}. The Oie horizon region-wide average Pb concentration and amount were both found to be significantly lower than those of the Oa horizon. Among individual sites, average Pb concentrations in their Oa horizons were significantly greater than Oie horizons for nine of the seventeen sites ($p < 0.05$) while the others were not significantly different. Oie horizon Pb amount ranged from 0.1 to 4.1 kg ha^{-1} with an average of 1.0 ± 0.1 kg ha^{-1} while Oa horizon Pb amount ranged from 0.2 to 8 kg ha^{-1} with an average of 3.3 ± 0.5 kg ha^{-1} (Fig. 3). Eight sites contained significantly higher Pb amount in their Oa horizon than in their Oi/Oe horizon ($p < 0.05$; Fig. 3) while the others were not significantly different. No sites had Oi/Oe horizons Pb concentrations above the USEPA Pb plant Eco-SSL of 120 mg kg^{-1} and only one central site had Oi/Oe horizons Pb concentrations above the USEPA Pb wildlife Eco-SSL of 56 mg kg^{-1} (Fig. 3). Two central sites had Oa horizons above the USEPA Pb plant Eco-SSL and seven sites had Oa horizons above the USEPA Pb wildlife Eco-SSL (Fig. 3).

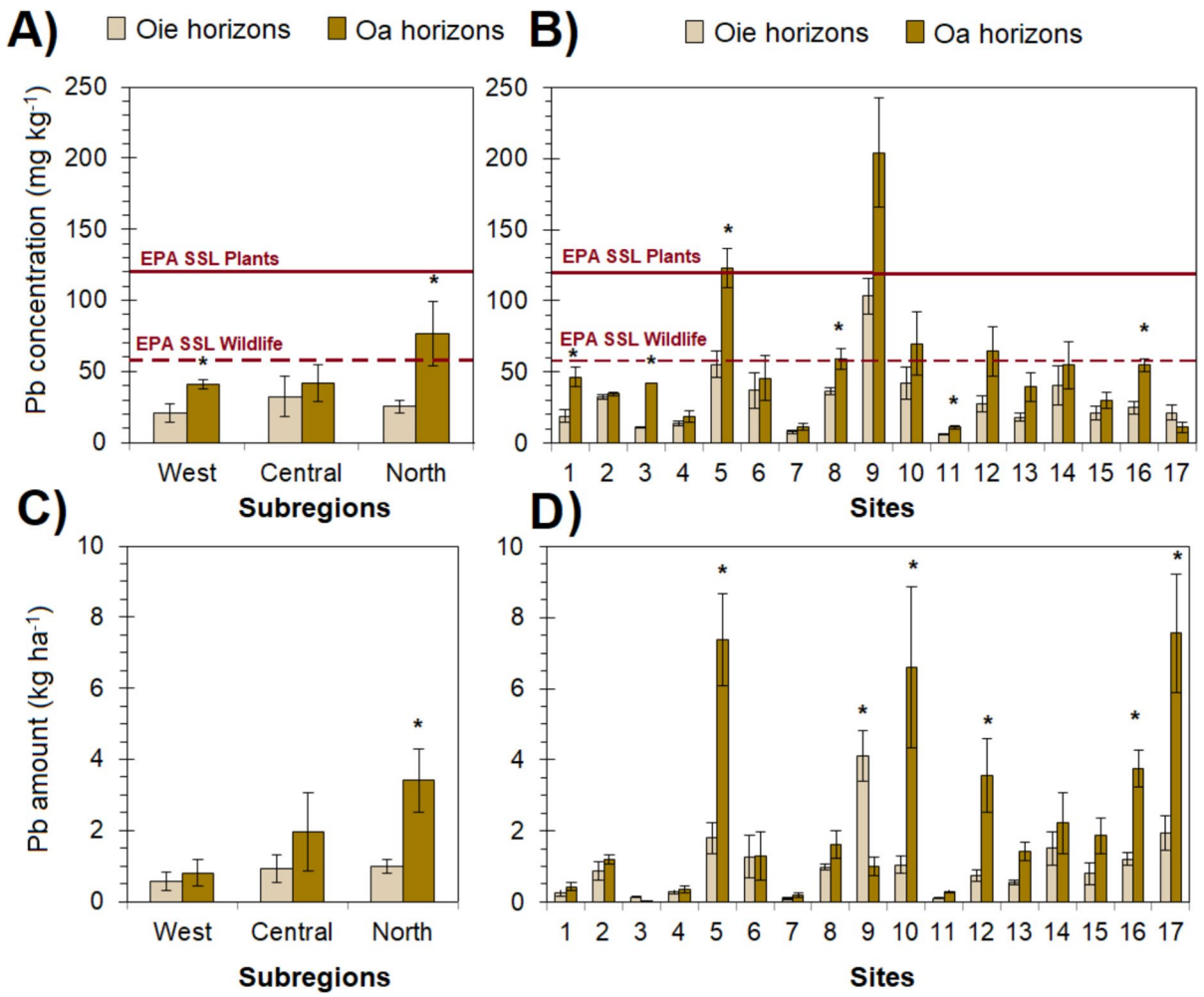

Fig. 3 Mean 2021 Oie and Oa concentrations and pools (± 1 standard error). 4 A Oie and Oa Pb concentrations by subregion and 4B for individual sites. 4C Oie and Oa Pb amounts grouped by subregion and 4D individual sites. (*) indicates a significant difference ($p < 0.05$) in Pb concentrations between Oie and Oa horizons using Wilcoxon rank sum test

Linear regressions found Oie and Oa Pb concentrations were correlated with some physicochemical properties (pH, Fe) and also less-specific geographic properties (latitude, longitude, elevation). Oie Pb concentrations were significantly correlated with latitude, longitude, and pH ($R^2 > 0.20$; $p < 0.05$; Supplemental Figure S3), while Oa Pb concentrations were significantly correlated with latitude, longitude, elevation, and pH ($R^2 > 0.20$; $p < 0.05$; Supplemental Figure S3). In terms of Pb amounts, the Oie horizons were significantly correlated with latitude, pH, and Fe amount ($R^2 > 0.20$; $p < 0.05$; Supplemental Figure S3), while the Oa horizons were significantly correlated with latitude, longitude, elevation, pH, and Fe amount ($R^2 > 0.20$; $p < 0.05$; Supplemental Figure S3).

3.3 Mineral Soil 2021 Sampling

Overall, mineral soil Pb concentrations were lower than the forest floor, varied among the three subregions, below hazardous concentrations, and decreased with depth. For the 2021 re-sampling, overall mineral soil Pb concentrations ranged from 5 to 71 mg kg^{-1} with an overall average of 14 ± 1 mg kg^{-1} across all depths and sites. Mineral soil Pb concentrations and amounts are provided at the site level in Supplemental Tables S3

and S4. Mean mineral soil Pb concentrations were significantly higher among western and central sites than among northern sites ($p < 0.05$) (Fig. 4). Overall mineral soil Pb amounts for the full soil profile (top 50 cm of soil) ranged from 11 to 53 kg ha^{-1} across all sites. No site had an average mineral soil Pb concentration above the EPA Eco SSL for plants of 120 mg kg^{-1} but site 3 had an average mineral soil 0 to 10 cm concentration above the wildlife EPA Eco SSL of 56 mg kg^{-1} (Fig. 4). The average mineral soil Pb amounts for individual depth intervals were found to be significantly higher than the average forest floor Pb amount ($p < 0.05$). Mean mineral soil Pb amounts were significantly higher among western and central sites than northern sites ($p < 0.01$; Supplemental Figure S4). Lastly, overall total mineral soil Pb pools (range: 6 to 53 kg ha^{-1}, average: 27.4 kg ha^{-1}; Supplemental Figure S4) were significantly greater than forest floor pools (range: 1 to 15 kg ha^{-1}, average: 4.1 kg ha^{-1}) ($p < 0.05$; Supplemental Figure S1).

Mineral soil physicochemical properties varied among sites and regions but only %SOM were associated with Pb concentrations, respectively. Across all sites, mineral soil samples were further analyzed for Pb and physicochemical properties for the following four depth intervals: 0–10 cm, 10–20 cm, 20–30 cm, and 30–50 cm (Fig. 4; Supplemental Table S3 and S4). Physicochemical properties of the mineral soils across all four depths: %SOM ranged between 4.5 to 28.5% with an average of 13 ± 4%, %Clay ranged between 3.3 to 31.6% with an average of 10.9 ± 2.1%, and lastly pH ranged between pH 2.7 to 4.7 with an average of pH 3.6 ± 0.2. These physicochemical properties varied significantly among the three regions. Mineral soil pH values were significantly higher

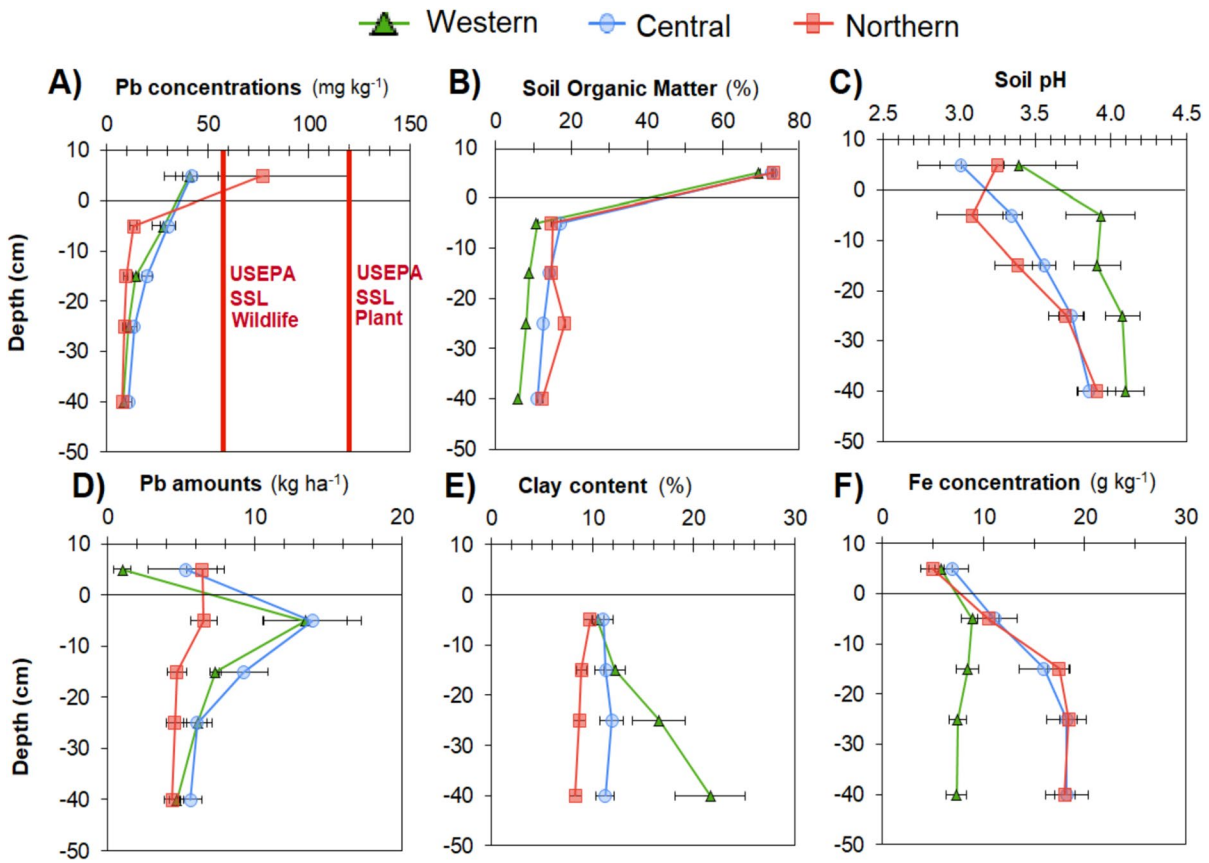

Fig. 4 Forest floor and mineral soil physicochemical properties of %clay content by hydrometer, %SOM by loss-on-ignition, soil pH by 1:2.5 soil to 0.1 M $CaCl_2$ solution, and Fe concentration by strong acid digestion

at western sites (4.0 ± 0.2) than central (3.6 ± 0.1) or northern sites (3.5 ± 0.1). Mineral soil %SOM concentrations were significantly lower at western sites (8.5% ± 0.8%) than central (14% ± 2%) or northern sites (15% ± 2%) ($p < 0.05$). Mineral soil %Clay was significantly greater at western sites (15% ± 2%) than central (11% ± 1%) or northern sites (9% ± 1%) ($p < 0.05$). Mineral soil Fe concentrations were significantly greater at central (16 ± 2 g kg^{-1}) and northern sites (16 ± 2 g kg^{-1}) than at western sites (8 ± 1 g kg^{-1}) ($p < 0.05$), particularly below the 0 to 10 cm depth interval (Fig. 4). The relationships among mineral soil Pb concentrations with physicochemical properties and geographic factors were examined across the seventeen sites for each depth interval using linear regressions, a stepwise regression and significant variables included in a multiple-regression (Table 2). Overall, mineral soil Pb concentrations were generally found to be significantly correlated with latitude, elevation, and %SOM (Supplemental Figure S5).

3.4 Forest Floor Desorption and Mineral Soil Sorption

The desorption of Pb from 2021 forest floor samples was determined using batch reactors under acidity (acid treatment), organic ligands of citrate and acetate (DOL treatment), and base cation salt treatments of Ca, Mg, K, and Na (salt treatment) and show a consistent pattern across the regions and relationships with %SOM and pH. The treatment DOL at pH 6.8 had the highest average Pb desorption% of all six treatments across all seventeen sites of 75% ± 11% (Fig. 5). When compared to the average forest floor Pb desorption by DI water control treatment (22% ± 6%), the treatments of acid, acid + DOL, and salt treatments did not significantly increase Pb desorption (Fig. 5). The two treatments salt + DOL and acid + salt + DOL were significantly greater than the control and acid treatments, but not the acid + DOL or salt treatments ($p < 0.01$; Fig. 5). Forest floor Pb desorption was aggregated among treatments and compared across the seventeen sites, which had an average of 41% ± 7% ranged from a low of 10% for Site

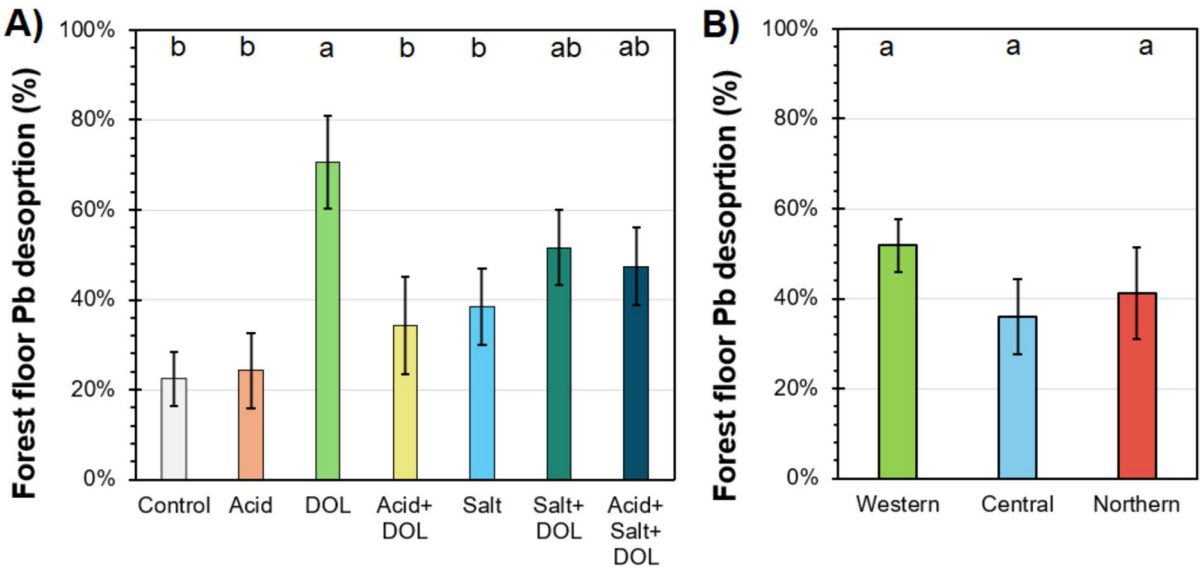

Fig. 5 Forest floor desorption experiment to determine impact of acidity, dissolved organic ligands (DOL), and base cation salts on release of Pb. In brief, three treatments were examined: acid (pH 3 nitric acid), DOL (50 mM citrate and 50 mM acetate at pH 6.8), and salts (50 mM Ca, 50 mM Mg, 50 mM K, and 50 mM Na solution at pH 6.8) in triplicate for forest floor (Oa material) from each of the seventeen sites. Each reactor was shaken horizontally for 48 h at 25 °C, settled for 12 h, centrifuged, and filtered to < 0.45 µm. Average Kd desorption for each treatment across the seventeen sites and across the three subregions. Letters indicate significant grouping, in which different letters indicate significant difference ($p < 0.05$) using Kruskal–Wallis test and post-hoc Wilcoxon rank-sum test

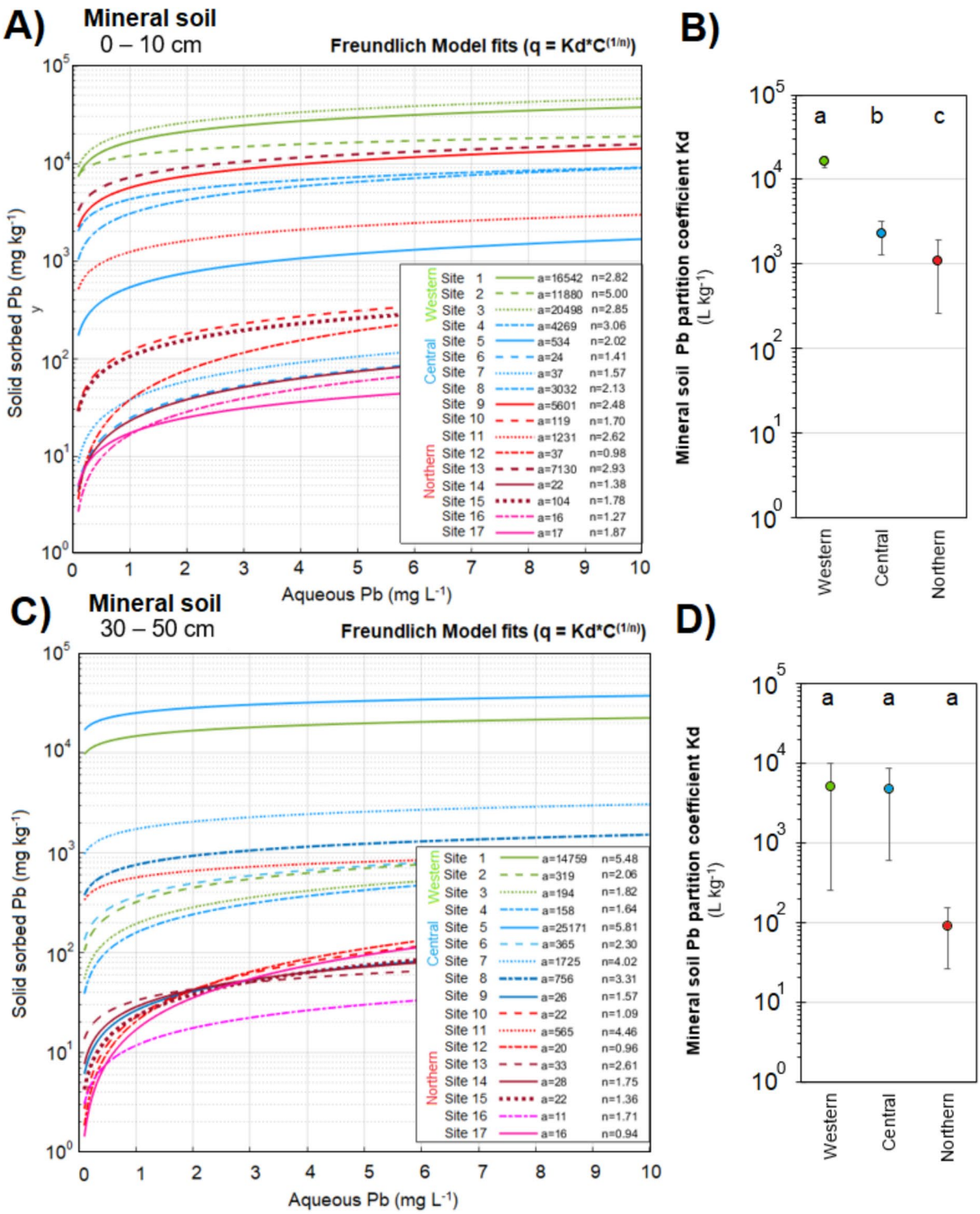

9 to a high of 75% for Site 3. Forest floor Pb desorption% did not vary significantly among the three subregions (Fig. 5). Forest floor Pb desorption% was not correlated with forest floor properties of Fe concentrations, thickness, elevation, precipitation, or MAT but was positively correlated with pH ($R^2 = 0.37$,

◂**Fig. 6** Mineral soil (0–10 cm and 30–50 cm) adsorption isotherms to determine partitioning coefficient (Kd) and fit parameter (n). In brief, $Pb(NO_3)_2$ at 0, 5, 50, 100, and 500 mg L^{-1} with 100 mg L^{-1} and diluted to four treatment levels in triplicate with 100 mg L^{-1} $NaNO_3$ to maintain ionic strength. Each reactor was shaken horizontally for 48 h at 25 °C, settled for 12 h, centrifuged, and filtered to < 0.45 µm. Average Kd values were compared across the three subregions and letter indicate significant grouping, in which different letters indicate significant difference ($p < 0.05$) using Kruskal–Wallis test and post-hoc Wilcoxon rank-sum test

$p < 0.01$) and negatively correlated with %SOM ($R^2 = 0.23$, $p < 0.05$).

Mineral soil Pb sorption was determined through adsorption isotherms using batch reactors for the 0–10 cm depth and 30 to 50 cm depth and overall mineral soil Kds were greater for western sites and associated with clay and site latitude. Freundlich model fit was strong for nearly all mineral soils studied with $R^2 > 0.95$ except for three mineral soils. Mineral soil Kd values had a large range from 0.7 up to 1.2×10^6 with overall medians of 534 L kg^{-1} for 0–10 cm and 33 L kg^{-1} for 30–50 cm (Fig. 6). Mineral soil Kd values were significantly greater for western sites (16307 ± 2491 L kg^{-1}) than central sites (2250 ± 978 L kg^{-1}) and northern sites (1085 ± 826 L kg^{-1}) for 0–10 cm depth ($p < 0.01$; Fig. 6). Mineral soil Kd values were not significantly different for western sites (5091 ± 4834), Central sites (4700 ± 4102 L kg^{-1}), or northern sites (90 ± 64 L kg^{-1}) for 30–50 cm depth (Fig. 6). Mineral soil 0–10 cm and 30–50 cm Kd values were not correlated with Fe concentrations, %SOM, pH, thickness, elevation, precipitation, or longitude. However, mineral soil 0–10 cm Kd values were negatively correlated with latitude ($R^2 = 0.36$, $p < 0.01$) and mineral soil 30–50 cm Kd values were positively correlated with %Clay ($R^2 = 0.34$, $p < 0.01$) and negatively correlated with latitude ($R^2 = 0.35$, $p < 0.05$).

3.5 Tree Foliage and Litterfall Pb Estimates for 2021 Sampling

Foliar Pb concentrations were measured for dominant tree species across the seventeen sites and three subregions in 2021 and show limited differences spatially across sites and regions and among genera. Similar measurements were not made in previous samplings and were collected to estimate modern accumulation and litterfall fluxes. Foliar Pb concentrations across all sites ranged from 0.4 to 2.3 mg kg^{-1} with an overall average of 0.8 ± 0.1 mg kg^{-1}. No significant differences in foliar Pb concentrations were observed between the three subregions, nor were any significant differences observed between sites located (Fig. 7). Estimated foliar Pb amounts ranged from 0.4 g ha^{-1} up to 9.1 g ha^{-1} did not vary among the subregions when comparing among western sites, central sites (2.1 ± 1.0 g ha^{-1}), and northern sites (1.6 ± 0.4 g ha^{-1}). Lastly, site averaged forest floor Pb concentrations, mineral soil Pb concentrations for each depth intervals, and pH, %SOM, mass or Fe concentrations were all poorly correlated with site averaged foliar Pb concentrations ($R^2 < 0.10$).

Using our estimated litterfall mass and foliar concentrations, we estimated annual litterfall fluxes for the seventeen sites. Our data estimated that litterfall Pb fluxes are significantly greatest at Site 2 and Site 14 and significantly lowest at Site 5, Site 13, and Site 15 ($p < 0.01$; Fig. 7). Our estimated litterfall Pb fluxes had mean values ranging from 1.5 to 4.0 g ha^{-1} yr^{-1} (Fig. 8) and were not vary significantly among the three subregions. Since foliar Pb concentrations were not significantly different among sites, the differences in litterfall fluxes are due to differences in tree canopy sizes with greater estimated canopies having greater leaf litter production. Litterfall Pb fluxes were not significantly correlated with forest floor Pb concentrations.

4 Discussion

4.1 Changes in Forest Floor Pb Through Time

The first objective of our study was to evaluate changes in forest floor Pb from 1980 to 2021 at seventeen long-term research sites set in three subregions of the northeastern US. Our results show that forest floor Pb concentrations from 1980 and 2011 have continued to decrease overall across the individual sites and across the three subregions (Fig. 1). The mean percent decrease in Pb concentration between 1980 and 2021 was greatest for western sites at $87 \pm 6\%$, followed by central sites at $73 \pm 6\%$, and then $65 \pm 3\%$ for northern sites. Despite having the middle rate of forest floor Pb concentration decreases, central sites had higher forest floor Pb concentrations

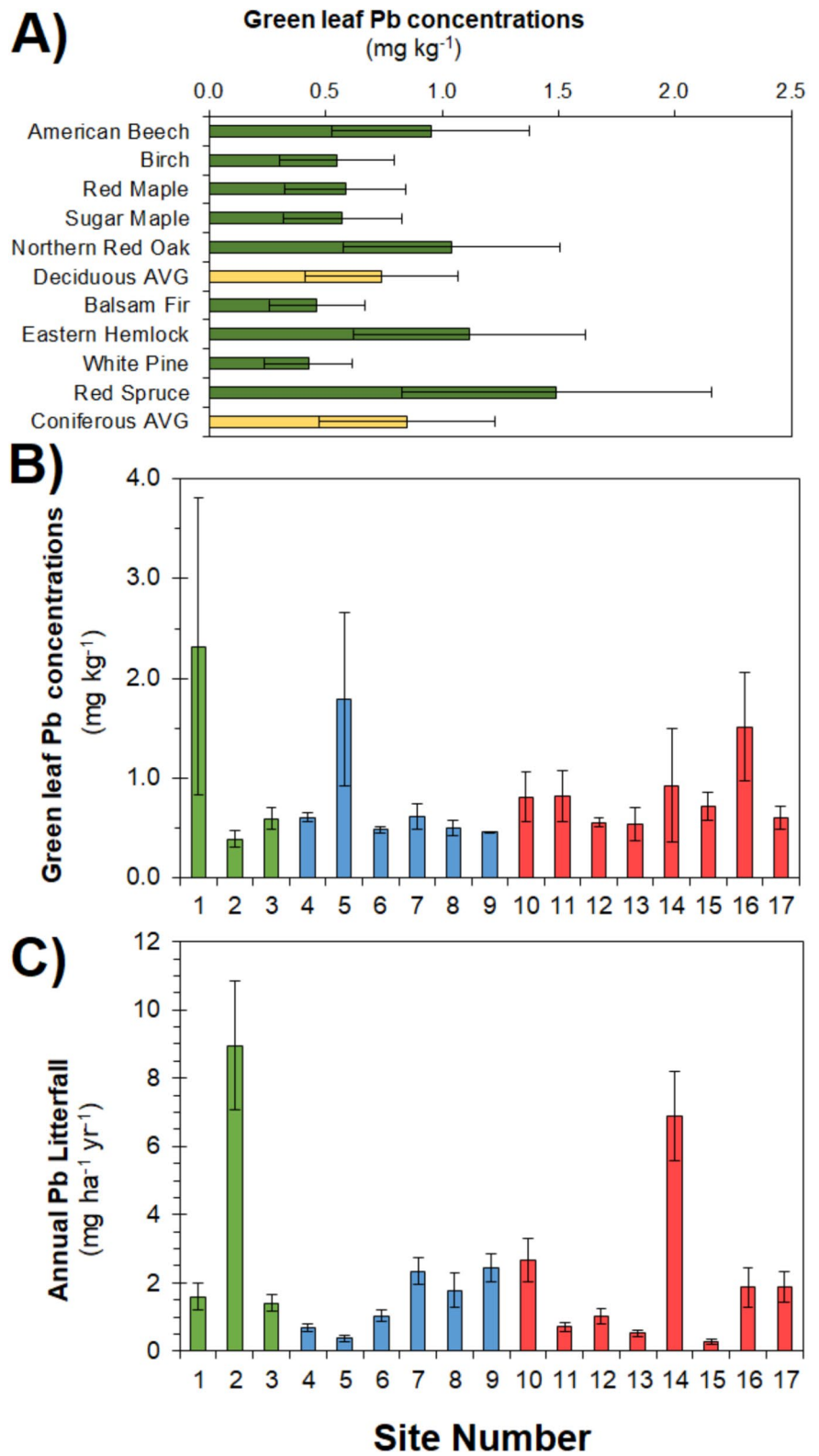

Fig. 7 Foliar Pb concentrations sampled as green leaves from dominant tree species from each of the seventeen sites. Mean concentrations ± 1 standard error. Deciduous AVG is the average of all deciduous trees across all sites and Coniferous AVG is the average of all coniferous trees across all sites

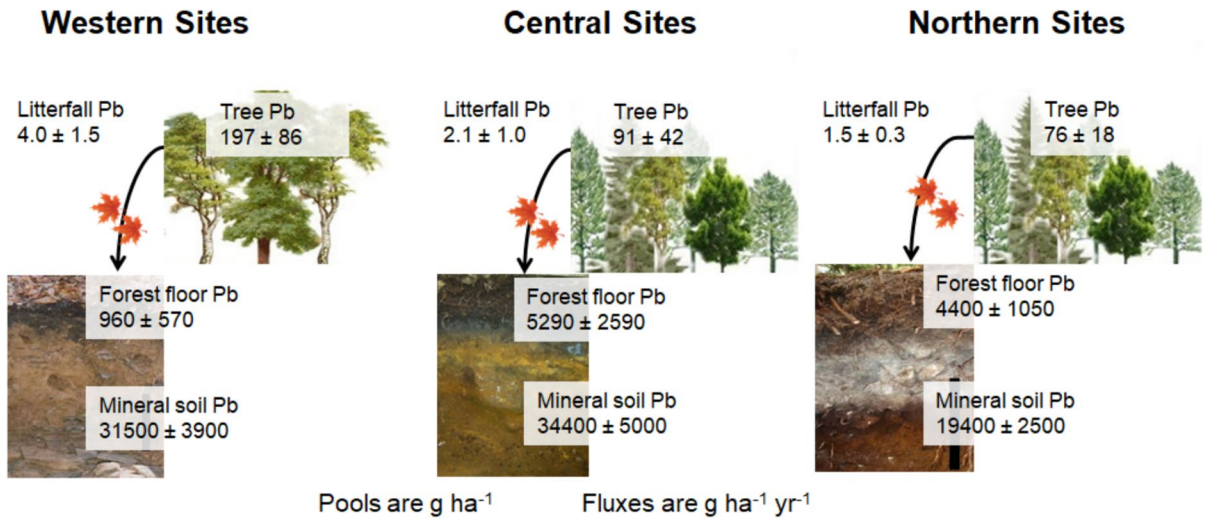

Fig. 8 Summary figure illustrating measured pools and estimated litterfall fluxes of Pb among the three subregions. Units for pools are g ha^{-1} and fluxes are g ha^{-1} $yr.^{-1}$

than northern and western sites (Fig. 1). These higher concentrations likely reflect both the original deposition pattern due to proximity to metropolitan urban centers (Johnson et al., 1982a, 1982b; Pouyat & McDonnell, 1991; Johnson and Richter, 2010) as well as higher %SOM in the forest floor at central and northern sites. Our calculations that include the most recent forest floor samples found the mean $T_{resp}C$, for all sites was 34 ± 4 yr, which was shorter than the Richardson et al. (2014) estimate of 46 ± 7 yr found in 2011. Increases in mean annual temperature and moisture could have affected the forest floor Pb inputs or storage Pb and organic matter in the forest floor (e.g. Feng et al., 2022; Zhao et al., 2024). However, our data set and observations are limited in identifying or quantifying the effects of multi-year or decadal changes in mean annual temperature or precipitation. Lastly, forest floor Pb concentrations at fourteen of the seventeen sites (82% of sites) were below USEPA ecological screening levels, 120 mg kg^{-1} for plants and 56 mg kg^{-1} for mammals, known to negatively impact plants and wildlife (Supplemental Figure S1; USEPA 2005). In contrast, forest floor Pb concentrations in 1980 had none of the seventeen sites (0%) were below both screening levels and only five sites below the 120 mg kg^{-1} plant screening level. This highlights that Pb concentrations have largely recovered and are generally unlikely to pose a hazard to wildlife but continued monitoring at Site 9 Mt. Everett in Massachusetts with > 150 mg kg^{-1} is warranted.

Changes in forest floor Pb amounts have continued to be more complex than forest floor Pb concentrations. Forest floor Pb amounts have decreased significantly across all sites when comparing the 1980 original sampling (15.6 ± 2.8 kg ha^{-1}) to the 2021 resampling (4.4 ± 1.1 kg ha^{-1}) (Fig. 1). Forest floor Pb amount response time ($T_{resp}A$) (35 ± 7 yrs) were not significantly different than $T_{resp}C$ (35 ± 5 yrs), suggesting that forest floor mass increased the variability within our data set but did not affect the calculated residence time of Pb in the forest floor. Quantifying decreases in forest floor Pb amounts has been difficult due to the spatial and potentially temporal variability in forest floor mass. Forest floor Pb amounts have exhibited greater heterogeneity in the forest floor material and total mass sampled each decade. These differences can stem from greater mineral soil A horizon inclusion with the forest floor Oa horizon and random sampling of microtopographic depressions (Friedland et al., 1992).

On the basis of faster changes in concentrations and amounts from 1980 to 2021, T_{respC} values, $T_{resp}A$ values, and previous isotopic data (Richardson et al., 2014), it can be concluded that the colder, thicker, and deeper forest floor at the northern sites are retaining Pb longer than the warmer, thinner, and shallower forest floor at western sites. Latitude, serving as a

proxy for mean annual temperature, was significantly correlated with forest floor Pb concentrations (Supplemental Figure S3) as well as $T_{resp}A$, which agrees with finds that litter decomposition rates can strongly control Pb and trace element retention (Stankwitz et al., 2012; Zhao et al., 2024). Thus, the colder mean annual temperature is partially responsible for the lower forest floor decomposition rate causing increased forest floor turnover times and Pb retention (Berg & Tamm, 1991; Dörr & Münnich, 1991; Johnson and Richter, 2010; Kaste et al., 2006; Schroth et al., 2008; Stankwitz et al., 2012; Zhao et al., 2024). Our observed correlations among forest floor thickness, forest floor mass, latitude, longitude, and mean annual precipitation all support the climate-vegetation-forest floor connectivity (Supplemental Figure S3). As temperatures and precipitation across the study region continue to increase along with extreme temperature anomalies (Basile et al 2025, 2023), the retention rate of Pb in the forest floor will likely decrease further. In conclusion, our findings show continued decreases in forest floor Pb concentrations and amounts, with varying levels of decreases and certainty, and greater changes in warmer areas of the study region.

4.2 Mechanism for Decreasing Forest Floor Pb

Decreasing forest floor Pb concentrations and amounts were hypothesized to be due to at least two processes: (1) dilution from the addition of new litter containing less Pb (Oie vs Oa) and (2) leaching from the forest floor to the underlying mineral soil (Friedland et al., 1992; Johnson and Richter, 2010; Kaste et al., 2006). Green leaf concentrations of Pb ranged from 0.4 to 1.5 mg kg^{-1} and thus is a low, non-negligible concentration (Fig. 7). These concentrations match other observations such as Watmough and Hutchinson (2004) who found Pb concentrations to be ~ 0.3 mg kg^{-1} in foliage in south-central Ontario, Canada. Similarly, Richardson et al. (2024) found that litterfall Pb concentrations from 2018 to 2023 across six sites ranging from Virginia to New Hampshire ranged from 0.3 to 0.8 mg kg^{-1}. Richardson et al. (2024) measured litterfall fluxes of 0.001 to 0.009 kg ha^{-1}, which is similar our current study estimates 0.002 to 0.004 kg ha^{-1} litterfall fluxes of Pb. Since our forest floor Pb amounts ranged from 0.7 to 16 kg ha^{-1}, these litterfall inputs may be considered negligible fluxes at < 1% of the current inventory present. Thus, the addition of new litter with low Pb concentrations is likely aiding the decrease in forest floor Pb via dilution.

For the second process of downward Pb leaching, Johnson et al., (1995), Kaste et al. (2003), and Richardson et al. (2014) demonstrated that Pb has moved from forest floor to mineral soil but were based upon synoptic sampling. From the desorption study we conducted, we found that dissolved organic ligand (DOL) complexation was the most important mechanism allowing forest floor Pb desorption and thus downward leaching. However, the effect of dissolved organic ligands is pH dependent as well-documented (Wu et al., 1999; Schwab et al., 2005; Zheng et al., 2022). The DOL treatment was circumneutral and thus the citrate and acetate ligands can effectively chelate Pb and increase Pb solubility (Schwab et al., 2005; Zhang et al., 2022). However, the acid treatment (acid, acid + DOL, acid + salts + DOL) had pH < 4.0 conditions matching forest floor pH, which causes protonation of DOL and limits chelation to the point of not being significantly greater than DI water and native soluble DOL. This matches findings by Zheng et al. (2022) in which competitive cations and acidity diminished the chelation of soil Pb and promoted its retention in soil. Across the forest floor desorption treatments of base cations for substitution from cation exchange sites, nitric acid for proton-desorption, and dissolved organic ligands for increase solubility, there was a mean of 41% ± 7% of Pb solubilized over the 60 h desorption experiment. This highlights that Pb is strongly-bound in the forest floor and downward leaching in dissolved forms can be as important but the majority of Pb could be not desorbed. Previous studies have shown a strong propensity of Pb sorption to organic and inorganic dispersible colloids < 0.002 µm in size and their ability to leach through soil (e.g. Löv et al., 2018; Tang et al., 2024; Zhang et al., 2005). In conclusion, our findings support both mechanisms of new litter dilution and downward leaching as important means of decreasing forest floor Pb concentrations and amounts, but it must be noted that Pb could be leached downward into the mineral soil via colloids, which were not investigated in this study.

4.3 Mineral soil Pb Concentrations and Amounts

Objective 2 was to evaluate mineral soil Pb in 2021 at the 17 research sites and 3 subregions and investigate variation in sorption across the region. Our mineral soil Pb concentrations are similar to those in other areas with extensive non-point source pollution. For example, Juřička et al. (2023) measured mineral soil Pb concentrations between ~ 5 to ~ 60 mg kg^{-1} in Czech Republic mountain forests. We acknowledge that without the use of Pb isotopes, the measured Pb in the mineral soil must be considered a mixture of pollutant Pb and geogenic Pb from mineral weathering (Kaste et al., 2003; Richardson et al., 2014). We have estimated the mineral soil Pb amount in the top 50 cm of soil across the seventeen sites were significantly greater amounts in western and central sites than northern sites ($p < 0.01$; Fig. 8). These differences are likely due to the deeper clay-rich soils at western and central sites compared to shallow, rocky soils at northern sites. From our stepwise and multiple regressions, mineral soil Pb concentrations were primarily positively correlated with latitude across depths, followed by longitude, elevation, Fe, and %SOM and negatively correlated with soil pH (Table 2). Positive associations between mineral soil Pb concentrations and amounts with soil Fe and %SOM indicate that soil development is increasing the amount of organic matter and secondary minerals both of which promote Pb accumulation. This matches findings from Juřička et al. (2023) studying Pb in Czech Republic mountain forest soils. The adsorption of Pb to organic matter has been well-documented in previous studies and reviews (Adriano 2001; Stefanowicz et al., 2020; Zeng et al., 2017). In particular, anionic functional groups such as carboxylate, alcohols, thiols, and amine groups within organic matter can complex Pb aiding in retention and insolubility (e.g. Wang et al., 2018; Zhang et al., 2022). Moreover, amorphous and crystalline Fe oxyhydroxides within the mineral soil can adsorb Pb on charge sites (Yang et al., 2022; Zheng et al., 2022), although this is pH dependent and markedly decrease below pH 4 (Strawn & Sparks, 2000; Wang et al., 2018; Zeng et al., 2017).

To examine the potential differences in mineral soil retention, we measured the partition coefficient Kd for two depths across the seventeen sites (Fig. 6). Surprisingly, mineral soil Kd for 0–10 and 30 to 50 cm depths were not significantly correlated with mineral soil Fe concentrations or %SOM which are commonly associated with sorption (e.g. Park et al., 2019; Zheng et al., 2022). Instead, mineral soil Kd were negatively correlated with latitude and positively correlated with clay content, confirming the clay-rich soils and less rocky young soils were able to adsorb Pb at greater rates (see Reimann et al., 2011). In conclusion, our findings show that mineral soil Pb concentrations and amounts follow expected trends of soil physicochemical properties governing mineral soil Pb sorption, but the partitioning to solid phase appears more related to pedogenesis based upon strong correlations with spatial variables of latitude.

4.4 Foliar and Litterfall Pb Varied Little with no Effect on Forest Floor Pb

In our last objective, we compared 2021 foliar Pb concentrations and predicted litterfall Pb fluxes with Oie vs Oa Pb concentrations and amounts across the 17 research sites, 3 subregions, and 8 sampled tree genera in order to evaluate the role of trees in biogeochemical cycling of Pb. We found that foliar Pb concentrations were not significantly different among sites nor among the dominant tree species. Foliar Pb concentrations (Fig. 7) were lower than ~ 7 mg kg^{-1} measured by Smith and Siccama (1981) at Hubbard Brook in New Hampshire showing 2021 tree leaves are accumulating less Pb due to reduced atmospheric capture of atmospheric Pb pollution. Thus, our data suggests the dominant source of Pb to trees in 2021 was uptake from forest floor and mineral soil, of either naturally sourced Pb weathered from bedrock or legacy Pb pollution. We expected that retention of pollutant Pb by tree uptake may prolong elevated Pb in the forest floor. However, our estimated litterfall Pb fluxes (< 1% of the current forest floor inventory present) were insignificant and not significantly correlated with forest floor Pb concentrations, which demonstrates that tree Pb uptake-forest floor pools storage is not enhanced due to legacy Pb pollution.

There were some differences within coniferous and deciduous trees as the highest and lowest foliar Pb concentrations were coniferous genera (Fig. 7). The lack of significant differences among three genera and between coniferous and deciduous foliar Pb concentrations were not expected as previous studies had shown significant differences in Pb concentrations

that can result from different exposure rates as well as different tree genera (Richardson & Friedland, 2016). For differences among the genera, we expected higher uptake rates for birch than other deciduous trees. In previous studies in the region found that foliar Pb concentrations were nearly double for birch (yellow and paper at 0.60 mg kg^{-1}) compared to other deciduous trees (American beech, sugar maple, red maple) (Richardson & Friedland, 2016). Our results (Fig. 7) do agree with Richardson and Friedland (2016) that found spruce had higher foliar Pb (0.36 mg kg^{-1}) than other deciduous trees (~28 mg kg^{-1}). Further, our foliar concentrations are significantly lower than other rural forest ecosystems experiencing on-going elevated Pb deposition such as the Tieshanping Forest Park in China with pine needle Pb concentrations reaching ~37 mg kg^{-1} (Zhou et al., 2019).

With respect to varying exposure levels, we expected sites with higher forest floor and/or mineral soil Pb concentrations to correspond with higher foliar Pb concentrations. However, regressions showed that forest floor, Oie, Oa, and mineral soil concentrations did not significantly correlate with site average foliar Pb concentrations (Supplemental Figure S3) or litterfall Pb amounts. This poor correlation highlights that other factors not examined in this study are controlling foliar Pb, such as root control and rhizosphere processes on Pb uptake (Albert et al., 2020; Liu et al., 2023; Rahman et al., 2024), tree genera or ecosystem factors affecting Pb uptake, or modern Pb atmospheric deposition rates directly to leaf surfaces. This agrees with low soil to leaves translocation factors of < 1.0 for most plants as described by Redovniković et al. (2017) and Kumar and Prasad (2018). In summary, our foliar Pb concentrations did not vary among three genera nor spatially, hinting at soil processes controlling Pb within trees and our estimated litterfall Pb fluxes does not support a feedback loop between forest floor Pb and tree leaf Pb.

5 Conclusions

Our study shows that Pb concentrations and amounts in the forest floor have decreased at these seventeen sites in the northeastern US.. The faster rates of decreasing forest floor Pb at western sites may be due to changes in climate (warmer, wetter) and biological activity (e.g. decreased litterfall trees due to pests or greater decomposition by soil biota). Forest floor Pb amounts (Pb mass per unit area) have also decreased significantly since 1980 and also since 2011, despite variability in forest floor mass. These results meet our expectations that Pb will continue to move downward into the mineral soil as a result of continued turnover of the forest floor despite its high sorption capacity for Pb. The forest floor Pb response times (*TrespC* and *TrespA*) were significantly correlated with the %SOM content and site latitude. This spatial relationship highlights that colder sites have slower turnover of the forest floor, promoting Pb retention.. Forest floor Pb desorption was greatest with the presence of organic ligands, but negatively impacted by acidity and competing base cations. The desorption experiment found a large proportion (~35 to 50% of Pb in the forest floor) can be solubilized by ligands, acidity, and base cation exchange. Lastly, forest floor and mineral soil Pb concentrations were generally below USEPA ecological screening levels known to negatively impact plants and wildlife and thus most sites do not warrant considerations for any active management for the pollutant Pb.

As expected, mineral soil Pb concentrations were comparable or lower than forest floor concentrations and associated with %SOM concentrations and Fe amounts. However, mineral soil Kd for Pb was only associated with latitude and not specific soil properties, which implies other factors not measured such as mineralogy, geology, or organic matter composition. Mineral soil Pb pools are much larger than the forest floor and varied across regions, with lowest Pb pools at northern sites, likely due to lowest rates of Pb migration from forest floor to mineral soil. Foliar Pb concentrations and amounts were not related to forest floor or mineral soil concentrations, demonstrating trees are discriminating against Pb uptake, which agrees with previous field and manipulation studies. Repeated study of forest soils at periodic time intervals across the region is needed to identify the ultimate fate of pollutant Pb and to determine impacts on terrestrial organisms, particularly birds, amphibians, and invertebrate predators.

Acknowledgements The authors thank Ivan C. Mischenko and Madelyn E. Metzler for field support and Paul Zeitz for technical and laboratory assistance.

Author Contributions **Justin B. Richardson**: Conceptualization, Methodology, Investigation, Writing – Original Draft,

Writing – Review and Editing, Data Visualization. **Owen C. Porter:** Methodology, Investigation, Writing – Original Draft, Writing – Review and Editing, Data Visualization. **Andrew W. Schroth**: Investigation, Writing – Original Draft, Writing – Review and Editing, Data Visualization. **Andrew J. Friedland**: Conceptualization, Methodology, Supervision, Project Administration, Investigation, Writing – Original Draft, Writing – Review and Editing. **James M. Kaste**: Conceptualization, Methodology, Investigation, Writing – Original Draft, Writing – Review and Editing, Data Visualization.

Funding This research was funded by the University of Massachusetts Amherst College of Arts and Sciences to Dr. Justin B. Richardson and a Porter Family Foundation award to Andrew J. Friedland.

Data Availability The authors declare that the data supporting the findings of this study are available within the paper, its supplementary information files, and the University of Virginia Data Management System LibraOpen Data.

Declarations

Ethics Approval Not applicable.

Consent for Publication Not applicable.

Competing Interests The authors declare no financial or non-financial interests.

References

Albert, Q., Baraud, F., Leleyter, L., Lemoine, M., Heutte, N., Rioult, J. P., Sage, L., & Garon, D. (2020). Use of soil fungi in the biosorption of three trace metals (Cd, Cu, Pb): Promising candidates for treatment technology? *Environmental Technology*. https://doi.org/10.1080/09593330.2019.1602170

Augusto, L., De Schrijver, A., Vesterdal, L., Smolander, A., Prescott, C., & Ranger, J. (2015). Influences of evergreen gymnosperm and deciduous angiosperm tree species on the functioning of temperate and boreal forests. *Biological Reviews, 90*, 444–466.

Berg, B., & Tamm, C. O. (1991). Decomposition and nutrient dynamics of litter in long-term optimum nutrition experiments: I. Organic matter decomposition in *Picea abies* needle litter. *Scandinavian Journal of Forest Research, 6*(1–4), 305–321.

Bogush, A. A., Stegemann, J. A., & Roy, A. (2019). Changes in composition and lead speciation due to water washing of air pollution control residue from municipal waste incineration. *Journal of Hazardous Materials, 361*, 187–199.

Caballero-Gómez, H., White, H. K., O'Shea, M. J., Pepino, R., Howarth, M., & Gieré, R. (2022). Spatial analysis and lead-risk assessment of Philadelphia, USA. *GeoHealth, 6*(3), Article e2021GH000519.

Crimmins, A.R., Avery, C.W., Easterling, D.R., Kunkel, K.E., Stewart, B.C. and Maycock, T.K., 2023. Fifth national climate assessment

Ding, K., Wu, Q., Wei, H., Yang, W., Séré, G., Wang, S., Echevarria, G., Tang, Y., Tao, J., Morel, J. L., & Qiu, R. (2018). Ecosystem services provided by heavy metal-contaminated soils in China. *Journal of Soils and Sediments, 18*, 380–390.

Dörr, H., & Münnich, K. O. (1991). Lead and cesium transport in European forest soils. *Water, Air, and Soil Pollution, 57*, 809–818.

Duruibe, J. O., Ogwuegbu, M. O. C., & Egwurugwu, J. N. (2007). Heavy metal pollution and human biotoxic effects. *International Journal of Physical Sciences, 2*(5), 112–118.

Feng, J., He, K., Zhang, Q., Han, M., & Zhu, B. (2022). Changes in plant inputs alter soil carbon and microbial communities in forest ecosystems. *Global Change Biology, 28*(10), 3426–3440.

Ferrari, J. B., & Sugita, S. (1996). A spatially explicit model of leaf litter fall in hemlock–hardwood forests. *Canadian Journal of Forest Research, 26*(11), 1905–1913.

Friedland, A. J., Johnson, A. H., & Siccama, T. G. (1984). Trace metal content of the forest floor in the Green Mountains of Vermont: Spatial and temporal patterns. *Water, Air, and Soil Pollution, 21*, 161–170.

Friedland, A. J., Craig, B. W., Miller, E. K., Herrick, G. T., Siccama, T. G., & Johnson, A. H. (1992). Decreasing lead levels in the forest floor of the Northeastern USA. *Ambio, 21*(6), 400–403.

Isen, A., Rossin-Slater, M., & Walker, W. R. (2017). Every breath you take—every dollar you'll make: The long-term consequences of the Clean Air Act of 1970. *Journal of Political Economy, 125*(3), 848–902.

Jenkins, J. C., Chojnacky, D. C., Heath, L. S., & Birdsey, R. A. (2003). National-scale biomass estimators for United States tree species. *Forest Science, 49*(1), 12–35.

Johnson, A. H., & Richter, S. L. (2010a). Organic-horizon lead, copper, and zinc contents of mid-Atlantic forest soils, 1978–2004. *Soil Science Society of America Journal, 74*(3), 1001–1009.

Johnson, A. H., Siccama, T. G., & Friedland, A. J. (1982). Spatial and temporal patterns of lead accumulation in the forest floor in the northeastern United States. *Journal of Environmental Quality, 11*, 577e580.

Johnson, C. E., Siccama, T. G., Driscoll, C. T., Likens, G. E., & Moeller, R. E. (1995). Changes in lead biogeochemistry in response to decreasing atmospheric inputs. *Ecological Applications, 5*(3), 813–822.

Juřička, D., Valtera, M., Novotný, R., Komendová, R., Černý, J., & Pecina, V. (2023). The influence of Norway spruce and European beech on the vertical distribution of Cd, Cu, Pb and Zn in temperate forest soils. *European Journal of Forest Research, 142*(2), 247–257.

Kabata-Pendias, A. and Mukherjee, A.B., 2007. Trace Elements of Group 14 (Previously Group IVa). Trace elements from soil to human, pp.351–380

Kaste, J. M., Friedland, A. J., & Stürup, S. (2003). Using stable and radioactive isotopes to trace atmospherically deposited Pb in montane forest soils. *Environmental Science & Technology, 37*(16), 3560–3567.

Kaste, J. M., Friedland, A. J., & Miller, E. K. (2005). Potentially mobile lead fractions in montane organic-rich soil horizons. *Water, Air, and Soil Pollution, 167*, 139–154.

Kaste, J. M., Bostick, B. C., Friedland, A. J., Schroth, A. W., & Siccama, T. G. (2006a). Fate and speciation of gasoline-derived lead in organic horizons of the northeastern USA. *Soil Science Society of America Journal, 70*(5), 1688–1698.

Ketterer, M. E., Lowry, J. H., Simon, J. J., Humphries, K., & Novotnak, M. P. (2001a). Lead isotopic and chalcophile element compositions in the environment near a zinc smelting–secondary zinc recovery facility, Palmerton, Pennsylvania, USA. *Applied Geochemistry, 16*(2), 207–229.

Kumar, A., & Prasad, M. N. V. (2018). Plant-lead interactions: Transport, toxicity, tolerance, and detoxification mechanisms. *Ecotoxicology and Environmental Safety, 166*, 401–418.

Levin, R., Vieira, C. L. Z., Rosenbaum, M. H., Bischoff, K., Mordarski, D. C., & Brown, M. J. (2021). The urban lead (Pb) burden in humans, animals and the natural environment. *Environmental Research, 193*, Article 110377.

Liu, X., Ju, Y., Mandzhieva, S., Pinskii, D., Minkina, T., Rajput, V. D., Roane, T., Huang, S., Li, Y., Ma, L. Q., & Clemens, S. (2023). Sporadic Pb accumulation by plants: Influence of soil biogeochemistry, microbial community and physiological mechanisms. *Journal of Hazardous Materials, 444*, Article 130391.

Löv, Å., Cornelis, G., Larsbo, M., Persson, I., Sjöstedt, C., Gustafsson, J. P., Boye, K., & Kleja, D. B. (2018). Particle-and colloid-facilitated Pb transport in four historically contaminated soils-speciation and effect of irrigation intensity. *Applied Geochemistry, 96*, 327–338.

Luyssaert, S., Raitio, H., Vervaeke, P., Mertens, J., & Lust, N. (2002). Sampling procedure for the foliar analysis of deciduous trees. *Journal of Environmental Monitoring, 4*(6), 858–864.

Miller, E. K., & Friedland, A. J. (1994). Lead migration in forest soils: Response to changing atmospheric inputs. *Environmental Science & Technology, 28*, 662–669.

Morales-Silva, T., Corrêa-Silva, B., & Faria, L. D. (2024). Lead bioaccumulation in herbivorous insects and parasitoids reared on plants grown in lead-contaminated soil under field conditions. *Entomological Communications, 6*, ec06028–ec06028.

Nadim, F., Zack, P., Hoag, G. E., & Liu, S. (2001). United States experience with gasoline additives. *Energy Policy, 29*(1), 1–5.

Park, H. J., Park, H. J., Yang, H. I., Park, S. I., Lim, S. S., Kwak, J. H., Lee, G. T., Lee, S. M., Park, M., & Choi, W. J. (2019). Sorption of Pb in chemical and particle-size fractions of soils with different physico-chemical properties. *Journal of Soils and Sediments, 19*(1), 310–321.

Peterson, E. K., Carsella, J., Varian-Ramos, C. W., Schiffer, T., Staples, S. K., & Diawara, M. (2024). Effects of lead (Pb) from smelter operations in an urban terrestrial food chain at a Colorado Superfund site. *Bulletin of Environmental Contamination and Toxicology, 112*(1), Article 17.

Pouyat, R. V., & McDonnell, M. J. (1991). Heavy metal accumulations in forest soils along an urban-rural gradient in southeastern New York, USA. *Water, Air, and Soil Pollution, 57*(1), 797–807.

PRISM Climate Group (2023). PRISM Climate Data. Northwest Alliance for Computational Science and Engineering-Oregon State University. https://prism.oregonstate.edu

Rahman, S. U., Qin, A., Zain, M., Mushtaq, Z., Mehmood, F., Riaz, L., Naveed, S., Ansari, M. J., Saeed, M., Ahmad, I., & Shehzad, M. (2024). Pb uptake, accumulation, and translocation in plants: Plant physiological, biochemical, and molecular response: A review. *Heliyon*. https://doi.org/10.1016/j.heliyon.2024.e27724

Redovniković, I. R., De Marco, A., Proietti, C., Hanousek, K., Sedak, M., Bilandžić, N., & Jakovljević, T. (2017). Poplar response to cadmium and lead soil contamination. *Ecotoxicology and Environmental Safety, 144*, 482–489.

Reimann, C., Smith, D. B., Woodruff, L. G., & Flem, B. (2011). Pb-concentrations and Pb-isotope ratios in soils collected along an east–west transect across the United States. *Applied Geochemistry, 26*(9–10), 1623–1631.

Richardson, J. B., & Friedland, A. J. (2016). Influence of coniferous and deciduous vegetation on major and trace metals in forests of northern New England, USA. *Plant and Soil, 402*, 363–378.

Richardson, J. B., Friedland, A. J., Kaste, J. M., & Jackson, B. P. (2014). Forest floor lead changes from 1980 to 2011 and subsequent accumulation in the mineral soil across the northeastern United States. *Journal of Environmental Quality, 43*(3), 926–935.

Richardson, J. B., Donaldson, E. C., Kaste, J. M., & Friedland, A. J. (2015). Forest floor lead, copper and zinc concentrations across the northeastern United States: Synthesizing spatial and temporal responses. *Science of the Total Environment, 505*, 851–859.

Richardson, J. B., Truong, M. T., & Dobson, A. M. (2024). Throughfall and litterfall fluxes reveal new inputs and foliar cycling maintain Pb, Cd, Cu, and Zn pollution legacy in eastern US temperate forests. *Pollutants, 4*(4), 474–489.

Sarkar, S., Ahmed, T., Swami, K., Judd, C. D., Bari, A., Dutkiewicz, V. A., & Husain, L. (2015). History of atmospheric deposition of trace elements in lake sediments, ~ 1880 to 2007. *Journal of Geophysical Research: Atmospheres, 120*(11), 5658–5669.

Schroth, A. W., Bostick, B. C., Kaste, J. M., & Friedland, A. J. (2008). Lead sequestration and species redistribution during soil organic matter decomposition. *Environmental Science & Technology, 42*(10), 3627–3633.

Schwab, A. P., He, Y., & Banks, M. K. (2005). The influence of organic ligands on the retention of lead in soil. *Chemosphere, 61*(6), 856–866.

Šerić Jelaska, L., Jurasović, J., Brown, D. S., Vaughan, I. P., & Symondson, W. O. (2014). Molecular field analysis of trophic relationships in soil-dwelling invertebrates to identify mercury, lead and cadmium transmission through forest ecosystems. *Molecular Ecology, 23*(15), 3755–3766.

Siccama, T. G., & Smith, W. H. (1978). Lead accumulation in a northern hardwood forest. *Environmental Science & Technology, 12*(5), 593–594.

Smith, W. H., & Siccama, T. G. (1981). The Hubbard Brook Ecosystem Study: Biogeochemistry of lead in the Northern Hardwood Forest. *Journal of Environmental Quality, 10*(3), 323–333.

Soil Survey Staff. 2022. Keys to Soil Taxonomy, 13th ed. USDA-Natural Resources Conservation Service

Stankwitz, C., Kaste, J. M., & Friedland, A. J. (2012). Threshold increases in soil lead and mercury from tropospheric deposition across an elevational gradient. *Environmental Science & Technology, 46*(15), 8061–8068.

Stefanowicz, A. M., Kapusta, P., Zubek, S., Stanek, M., & Woch, M. W. (2020). Soil organic matter prevails over heavy metal pollution and vegetation as a factor shaping soil microbial communities at historical Zn–Pb mining sites. *Chemosphere, 240*, Article 124922.

Strawn, D. G., & Sparks, D. L. (2000). Effects of soil organic matter on the kinetics and mechanisms of Pb(II) sorption and desorption in soil. *Soil Science Society of America Journal, 64*(1), 144–156.

Tang, L., Gao, W., Lu, Y., Tabelin, C. B., Liu, J., Li, H., Yang, W., Tang, C., Feng, X., Jiang, J., & Xue, S. (2024). The formation of multi-metal (loid) s contaminated groundwater at smelting site: Critical role of natural colloids. *Journal of Hazardous Materials, 471*, Article 134408.

Ter-Mikaelian, M. T., & Korzukhin, M. D. (1997). Biomass equations for sixty-five North American tree species. *Forest Ecology and Management, 97*(1), 1–24.

Tuccillo, M. E., Blue, J., Koplos, J., Kelly, J., & Wilkin, R. T. (2023). Complexities in attributing lead contamination to specific sources in an industrial area of Philadelphia, PA. *Heliyon*. https://doi.org/10.1016/j.heliyon.2023.e15666

[USEPA] US Environmental Protection Agency. 2005. Ecological soil screening levels for lead: Interim final. Office of Solid Waste and Emergency Response, USEPA, Washington, DC. OSWER Directive 9285.7-70.

Wade, A. M., Richter, D. D., Craft, C. B., Bao, N. Y., Heine, P. R., Osteen, M. C., & Tan, K. G. (2021). Urban-soil pedogenesis drives contrasting legacies of lead from paint and gasoline in city soil. *Environmental Science & Technology, 55*(12), 7981–7989.

Walsh, D. C., Chillrud, S. N., Simpson, H. J., & Bopp, R. F. (2001). Refuse incinerator particulate emissions and combustion residues for New York City during the 20th century. *Environmental Science & Technology, 35*(12), 2441–2447.

Wang, Q., Wang, B., Lee, X., Lehmann, J., & Gao, B. (2018). Sorption and desorption of Pb (II) to biochar as affected by oxidation and pH. *Science of the Total Environment, 634*, 188–194.

Watmough, S. A., & Hutchinson, T. C. (2004). The quantification and distribution of pollution Pb at a woodland in rural south central Ontario, Canada. *Environmental Pollution, 128*(3), 419–428.

Wei, J., Li, H., & Liu, J. (2022). Heavy metal pollution in the soil around municipal solid waste incinerators and its health risks in China. *Environmental Research, 203*, Article 111871.

Yang, Z., Gong, H., He, F., Repo, E., Yang, W., Liao, Q., & Zhao, F. (2022). Iron-doped hydroxyapatite for the simultaneous remediation of lead-, cadmium- and arsenic-co-contaminated soil. *Environmental Pollution, 312*, Article 119953.

Zeng, G., Wan, J., Huang, D., Hu, L., Huang, C., Cheng, M., Xue, W., Gong, X., Wang, R., & Jiang, D. (2017). Precipitation, adsorption and rhizosphere effect: The mechanisms for phosphate-induced Pb immobilization in soils—a review. *Journal of Hazardous Materials, 339*, 354–367.

Zhang, M., Li, W., Yang, Y., Chen, B., & Song, F. (2005). Effects of readily dispersible colloid on adsorption and transport of Zn, Cu, and Pb in soils. *Environment International, 31*(6), 840–844.

Zhang, W., Jiang, F., & Sun, W. (2021). Investigating colloid-associated transport of cadmium and lead in a clayey soil under preferential flow conditions. *Water Science and Technology, 84*(9), 2486–2498.

Zhang, H., Zhang, R., Lu, T., Qi, W., Zhu, Y., Lu, M., Qi, Z., & Chen, W. (2022). Enhanced transport of heavy metal ions by low-molecular-weight organic acids in saturated porous media: Link complex stability constants to heavy metal mobility. *Chemosphere, 290*, Article 133339.

Zhao, X., Zang, F., Li, N., Huang, F., Chang, Y., & Zhao, C. (2024). Dynamics of trace elements during litter decomposition in a temperate forest as a function of elevation and canopy coverage. *Biogeochemistry, 167*(1), 39–57.

Zheng, Y., Li, Y., Zhang, Z., Tan, Y., Cai, W., Ma, C., Chen, F., & Lu, J. (2022). Effect of low-molecular-weight organic acids on migration characteristics of Pb in reclaimed soil. *Frontiers in Chemistry, 10*, Article 934949.

Zhou, J., Du, B., Wang, Z., Zhang, W., Xu, L., Fan, X., Liu, X., & Zhou, J. (2019). Distributions and pools of lead (Pb) in a terrestrial forest ecosystem with highly elevated atmospheric Pb deposition and ecological risks to insects. *Science of the Total Environment, 647*, 932–941.

Wu, J., Hsu, F.C. and Cunningham, S.D., 1999. Chelate-assisted Pb phytoextraction: Pb availability, uptake, and translocation constraints. Environmental Science & Technology, 33(11), pp.1898-1904.

Adriano, D.C., 2001. Trace elements in terrestrial environments: biogeochemistry, bioavailability, and risks of metals (Vol. 860). New York: Springer.

Basile, S., Crimmins, A., Lipschultz, F., Kunkel, K.E., Marvel, K., Terando, A., Tebaldi, C., Pierce, D., Su, W., Leung, L.R. and Hayhoe, K., 2025. Projections of future climate for US national assessments: past, present, future. Climatic Change, 178(4), pp.1-21.

Dewitz, J., 2021. National land cover database (NLCD) 2019 products (ver. 3.0, February 2024). US Geological Survey (USGS) Data Release, p.624.